energies

Review

Partial Discharges Monitoring for Electric Machines Diagnosis: A Review

Jonathan dos Santos Cruz [1,*], Fabiano Fruett [1], Renato da Rocha Lopes [1], Fabio Luiz Takaki [2], Claudia de Andrade Tambascia [2], Eduardo Rodrigues de Lima [2] and Mateus Giesbrecht [1]

1 School of Electrical and Computer Engineering, University of Campinas, Campinas 13083-970, Brazil
2 Eldorado Research Institute, Campinas 13083-898, Brazil
* Correspondence: j264527@dac.unicamp.br

Abstract: Online monitoring of Partial Discharges (PDs) in rotating electrical machines is an useful tool for machine prognosis, as it presents reduced costs compared to intrusive inspections and is associated with relevant problems. Although this monitoring method has been developed for almost 50 years, the recent advancements in processes automation and signal processing techniques allow improvements that are still being studied by academic and industrial researchers. To analyze the current context of PDs monitoring, this article presents a literature review based on concepts of PDs in rotating machines, data acquisition techniques, state-of-the art commercial equipment, and recent methodologies for detection and pattern recognition of PDs. The challenges identified in the literature that motivate the development of more reliable and robust PD monitoring systems are presented and discussed.

Keywords: partial discharge; rotating machine; monitoring; motor; generator; machine; machine learning; deep learning; PWM; inverter

check for updates

Citation: Cruz, J.d.S.; Fruett, F.; Lopes, R.d.R.; Takaki, F.L.; Tambascia, C.d.A.; Lima, E.R.d.; Giesbrecht, M. Partial Discharges Monitoring for Electric Machines Diagnosis: A Review. *Energies* **2022**, *15*, 7966. https://doi.org/10.3390/en15217966

Academic Editor: Hazlee Azil Bin Illias

Received: 22 September 2022
Accepted: 12 October 2022
Published: 27 October 2022

1. Introduction

The world energy matrix has been transformed and diversified since the industrial revolution. Global energy consumption is supplied by primary sources such as modern biofuels, solar, wind, hydropower, nuclear, natural gas, oil, coal, biomass, and other renewable energies. In 2021, this consumption totalled 176,431 TWh. The most significant contribution from generation came from sources such as winds, hydropower, nuclear, natural gas, oil, coal, and biomass, which corresponded to a total of 170,215 TWh [1]. The majority of these sources can be converted into electrical power using rotating electrical machines. These machines are also used as motors to convert electrical power into mechanical power in the industry, commerce, and residences. Since these machines work in high-demand environments, great operational reliability is needed. Premature machine failures in these environments can cause substantial economic losses, either through process breakdowns or physical damage to assets [2].

In high-demand plants, the machines work under intense stresses, also known as TEAM stresses, which means Thermal, Electrical, Environmental, and Mechanical tensions that result in the structural wear of the assets [3,4]. In these plants, the rotating electrical machines can work as generators or motors. A rotating electrical machine has two main structures, defined as a stator and a rotor. In most generators, the stator conducts most of the electrical energy converted from the mechanical energy, hence its importance. From [5], it is possible to verify that in turbo generators, stator failures correspond to 23% of the total, while for rotor failures and other types, the percentage is 14% and 63%, respectively. In hydro generators, the stator winding insulation is the structure with the most defects identified. In electric motors, stator, rotor, and other types of failures corresponded to 36%, 9%, and 55%, respectively, with a great amount of stator failures associated with insulation degradation.

Given the statistics presented, it is possible to verify that the field of study related to the development of faults diagnosis techniques in rotating electrical machines is broad. This has attracted increasing attention from researchers and companies, with the diagnosis being realized based on data collected for different operating conditions of the machine in different domains of analysis [6,7].

The predominant wearing factor is electrical, mainly associated with high intensity of partial discharges in the stator winding. Partial Discharges (PDs) are small electrical current discharges of short duration caused by the localized dielectric breakdown of a small region of the winding insulation system [8–10].

The constant activity of PDs contributes drastically to the degradation of the stator winding insulation, and can eventually lead to failures. The early diagnosis of the occurrence of PDs is essential so that it is possible to analyze the quality of the winding insulation system, especially for medium- and high-voltage units, due to the high costs associated with these assets [11]. As a result, asset monitoring through PD analysis is essential to implement adequate maintenance planning.

PDs can be measured using several signal domains, including electrical, thermal, mechanical (acoustic and inertial), magnetic, optical, and chemical. Electrical methods are the most used and also commercially explored. Non-electrical methods generally complement consecrated electrical methods.

Faced with the challenges and solutions presented in the last decade by the development of PD monitoring systems, this study presents a bibliographic review of concepts, commercial equipment, measurement techniques, and identification of PDs. The literature search was performed on Scopus, which is the largest database of abstracts and citations of articles from peer-reviewed scientific journals and conferences. The most recent studies that presented techniques with good performance in the acquisition, analysis, and interpretation of data were selected. In addition, topics that are relevant but receive little treatment in the literature were also selected, as follows: the influence of the drive system in the measurement of data and the location of PDs in windings, since a robust system with high reliability needs to consider these two factors.

To develop the study, in Section 2 the previous reviews of PDs in rotating machines are presented. In Section 3 the basic principles of PDs are described. Then, in Section 4, a review of commercial equipment used for PD detection is presented. Section 5 is dedicated to the state of the art in PD measurements. In Section 6, directions for further developments, including some improvements necessary to implement a robust system, are discussed. Finally, in Section 7, the conclusions are presented.

2. Previous Reviews

The development of PD monitoring systems in the context of rotating electrical machines requires a general study of the subject, since it involves concepts and methods based on very complex hardware and software. During the last few years, several studies on the subject have been developed. However, the compilation of the techniques used, and possible problems identified in these studies, are still rarely discussed.

In [12], a historical background on PD measurements from the 1940s was presented, in addition to important points such as a superficial description of components and basic methods for measuring and analyzing PDs, used from the 1940s to the 1970s. The problems of credibility of PD measurements associated with noise, PD indicators, sensor reliability, machine insulation life, and incorrect identification of fault causes have also been commented on superficially. The study also presents the state of the art of methods for noise suppression, identification of deteriorated winding insulation, and the indication of improvements to make the system more reliable.

An overview of the basic characteristics of PDs, such as types, causes, features, and risks, is discussed in [13]. The study describes pulse propagation modes of PDs and installation configurations of capacitive sensors and current transformers for data collection. Statistical-based signal filtering and time domain analysis methods are also discussed. For pattern recognition, supervised and unsupervised machine learning techniques are presented. In addition, suggestions for improvements were also discussed.

In [14], a brief review of PDs in rotating machines driven by inverters is presented, and the effects of inverter voltage waveform characteristics on the formation of PD patterns, such as rise time, pulse width and frequency, and the number of inverter levels, are discussed. Methodologies for detecting PDs are also described.

In [12,13], themes such as the importance of setting the threshold of PDs that indicate abnormality during machine operation considering the characteristics of each machine, the influence of machine drive systems on PD detection, and the exact location of PD sources in the stator winding of machines, are not discussed. In [14], only the influence of the drive system on the detection of PDs is discussed. These discussions are very important for obtaining robust and reliable systems. With this in mind, this study discusses all these themes and presents an overview of PDs based on standards, current commercial equipment, and modern pattern recognition techniques for detecting PDs. The importance of carrying out a new review of PDs in rotating machines comes from the fact that the last general review was carried out 5 years ago, as well as the need to bring current issues to debate.

3. Basic Principles of PDs

3.1. Characteristics of Stator Winding Insulation

The main functions of the stator winding insulation system are to prevent short circuits from occurring, to transfer heat from the conductor to a heat sink, and to prevent the conductors from vibrating due to the high electromagnetic forces [15]. For machines operating above 1 kV, preformed coils are designed and manufactured, which have insulating materials in different regions [15,16]. Understanding of these regions of the stator winding is of fundamental importance to identify PDs characteristics and their relationship with insulation defects [16]. Figure 1 shows some components of the double-layer stator winding of typical machines with windings of the type multi-turn coil and Roebel bar.

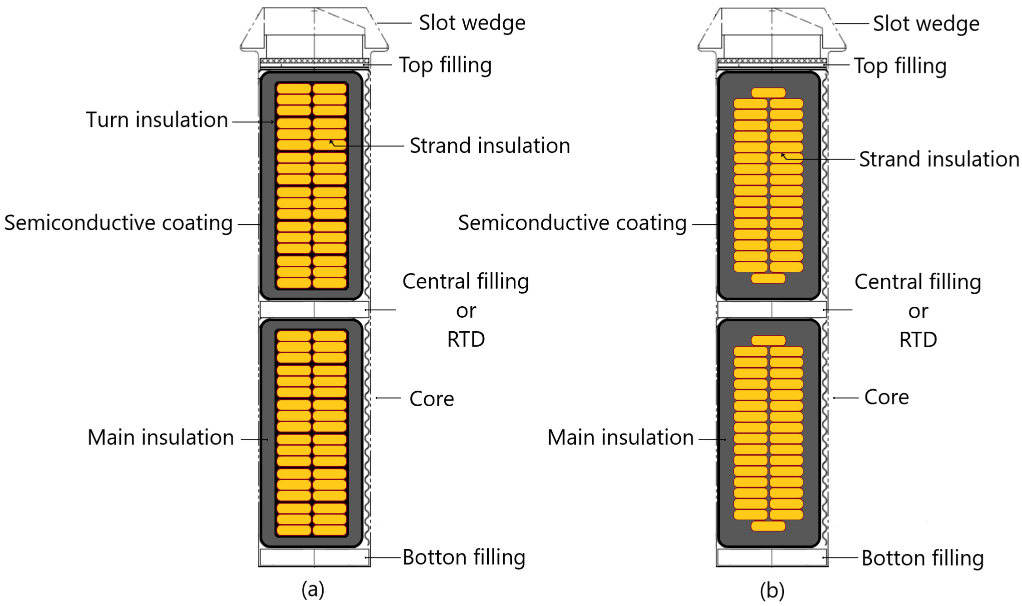

Figure 1. Cross-section of a slot (**a**) multi-turn coil and (**b**) Roebel bar.

In Figure 1, the strand insulation, which insulates the individual conductors, is responsible for reducing the skin effect, the turns insulation prevents the short circuit between them, the main insulator isolates the coils from the stator core, and the semiconductive coating is responsible for potential equalization in the slot [15].

Figure 2 illustrates the end-winding with the regions indicated numerically, and their insulation indicated by letters emphasizes a very important component of the stator winding, which does not appear in Figure 1: the layer of stress grading, also known as the field relief layer or semiconductive layer, which is responsible for controlling the electric field at the ends of the stator [17].

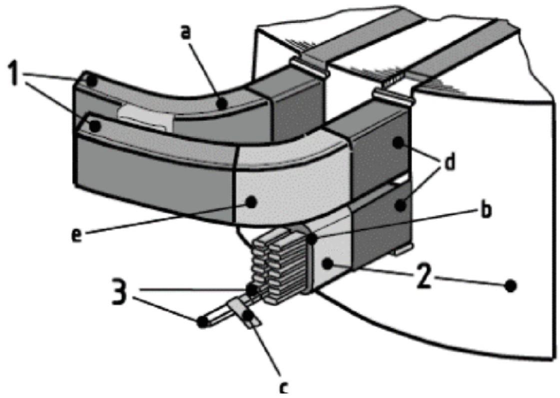

1- phase-to-phase
2- phase-to-ground
3- turn-to-turn
a- end-winding insulation
b- main insulation
c- turn insulation
d- semiconductive coating
e- stress grading layer

Figure 2. Preformed stator winding, adapted from [16].

Windings of electrical machines in industrial plants are generally subjected to high frequency and high peak current impulses due to PD activity, resulting in high electrical stress in regions of the winding, such as between coils of different phases, between a coil and the stator core or between turns of a coil deposited on the winding. In the sequel, we describe the causes and types of PDs in more detail.

3.2. Types of PDs

PDs occur due to high voltage stress on the stator winding insulation. The electrical stress in regions of void spaces or cavities within the insulation or on its surface will break the cavity dielectric, causing a discharge that will degrade the winding if not corrected [9,15].

In the IEC 60034-27 standard [18], PDs were divided into four categories, namely: internal discharges (due to voids or delamination in the insulation), slot discharges, end-winding surface discharges, and discharges due to conductive particles.

The types of PDs defined above and their respective regions of occurrence are shown in Figure 3. The figure shows an axial section of a stator slot of a typical machine, where it is possible to verify the formation of voids in the main insulation, delamination between the main insulation and the conductor insulation, discharges in the grading region, and end-winding discharges due to contamination.

3.2.1. Internal Discharges

Internal discharges develop within the electrical insulation of the stator winding and may be caused by the formation of internal voids and delamination in the insulation of the conductors or due to delamination between the conductor insulation and the main insulation. Discharge occurs because the cavities are subjected to high electrical stress that exceeds their dielectric strength.

Internal Voids

Internal voids occur due to the creation of internal cavities (approximately spherical bubbles) in the insulating material during the manufacturing process [18,19].

Internal Delamination

Internal delamination has an ellipsoidal geometric shape and can be caused during the manufacturing process due to imperfect curing (failure in resin hardening process) or by mechanical or thermal stress during the operation [18,19].

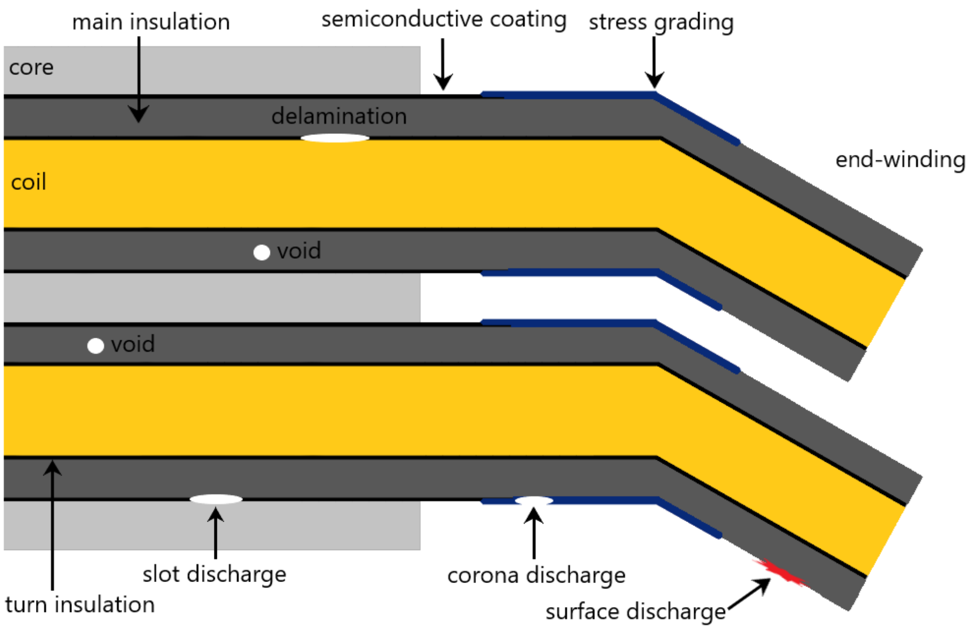

Figure 3. PD sources in the isolation system of a typical machine.

Delamination between Conductor Insulation and Main Insulation

They result from overheating, high mechanical forces [19], and also the different Coefficients of Thermal Expansion (CTEs) of the materials involved.

3.2.2. Slot Discharges

They develop between the coil and the stator core when insulation is compromised. These discharges can occur due to the increase in the local electric field in the semiconductive layer impurities or due to the movement of loose coils [19].

3.2.3. End-Winding Surface Discharges

They result from high electric field strengths in some areas of the end-winding due to defects in the grading layer caused by contamination, porosity, thermal effects, and even design errors [19].

3.2.4. Conductive Particle Discharges

Occur on the surface of the insulation of the stator coil, and are caused by contamination by conductive particles, can be of high intensity [19].

3.3. Most Usual Sensors for PD Detection

The occurrence of a PD is evidenced by electrical pulses, Radio Frequency (RF) pulses, acoustic emission, and optical emission [20]. In the literature, there is a predominance of online methods that analyze electrical pulses due to the ability to detect PDs inside and outside the insulation, in addition to the possibility of applying denoising methods. In some cases, the methods that analyze other PD evidences are used only as a complementary detection tools [20], since the analysis of RF pulses and acoustic emissions can suffer great external interference, resulting in a low Signal-to-Noise Ratio (SNR). For optical emissions, it is only possible to identify external discharge, since the internal discharge would not be visible. Based on the explanation above, this paper emphasizes conventional methods of electrical pulse analysis.

In the standards and technical literature, two types of sensors have been used to measure PDs, namely capacitive sensors and current transformers, with a predominance of the first ones. The configuration with sensors coupled to the terminals of the machines is most commonly used to perform the online PD detection. It is described in IEEE 1434 [20].

3.3.1. Capacitive Sensors

In the literature, there are three configurations for installing capacitive sensors on machines terminals, which are defined as simple, directional, and differential, as shown in Figure 4. The simple one uses only one sensor per phase, installed on the phase terminals of the machines, making this configuration more sensitive to noise, as it does not allow common-mode noise cancelation. The directional configuration uses two sensors per phase, with one sensor closer to the phase terminal and the other on the machines output bus, at least 2 m away. In this format, the external noise is separated from the PD signal based on the PD pulse arrival time analysis [13]. The differential configuration is recommended for machine designs with multiple circuits per phase and circuit rings, usually adopted in hydro generators, where couplers are installed at the stator circuit ring. If the noise comes from the external environment, it will enter the circuit rings, split, and propagate in both directions. If the circuit ring has the same length on both the left and right of the terminals, the pulse will arrive at the couplers at the same time, and if the conductors connecting the couplers to the analyzer are the same length, the signals will arrive simultaneously. In this case, the analyzer will interpret the signal as noise and not as a PD. In the case of asymmetrical circuit rings, it is possible to calibrate the cable lengths of the capacitive couplers to compensate for the different travel times in the different circuit rings. With this methodology, the pulse arrival time can be used for noise separation from the PD signal [21]. In Figure 4, it is possible to verify the three configurations.

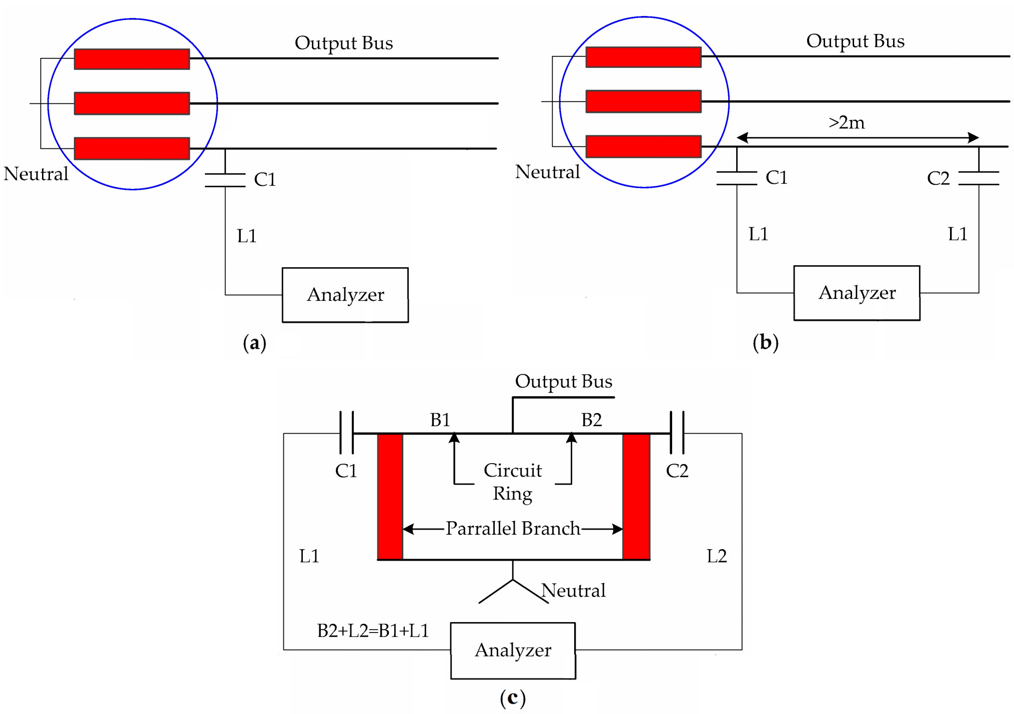

Figure 4. Configurations (**a**) simple, (**b**) directional and (**c**) differential, adapted from [13].

3.3.2. High Frequency Current Transformers (HFCT)

HFCT sensors are generally installed on each phase inside the terminal box to intercept PD current from rotating machines [22]. However, some methodologies use current transformers in the machines grounding system in the neutral ground connection [23]. Figure 5 presents the coupling forms.

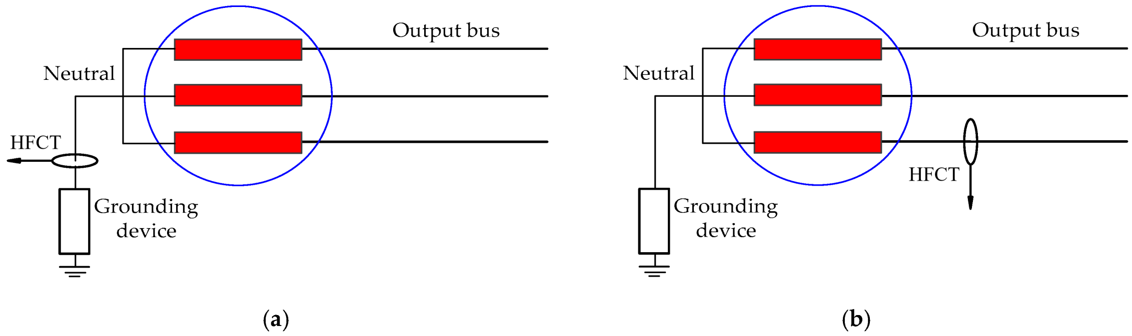

Figure 5. Configurations (**a**) neutral ground connection, (**b**) terminal, adapted from [13].

The PD measurement can be carried out using any of the mentioned sensors. However, it is recommended to follow international guidelines to perform consistent PD measurements. IEC 60034-27 [18] is commonly used as a reference in PD measurements, where only the use of capacitor sensors for PD data collection is specified.

3.4. Measurements of PDs

The PD measurement of stator windings can be carried out offline and online. Offline measurement requires the aid of an external voltage source when the machine is disconnected from the power system, while online measurement can be performed when the machine is operating normally and connected to the power system [24].

3.4.1. Offline Measurement

Offline PD measurements are performed by applying an external high-voltage source during routine and factory tests [25,26]. IEC 60034-27 [18] recommends that the PD measurement in offline tests on the stator winding must be in the low-frequency range, below 3 MHz, due to the capacitive and inductive nature of the winding. Another reason for performing the test in low frequency is that, depending on the location of the sensor relative to the PD source, the high-frequency components of the PD signal induced by the external high voltage source are likely to be attenuated. Therefore, the greater the detection frequency range, the greater the PD detection accuracy [27–31].

3.4.2. Online Measurement

Online measurements of PDs are taken during commissioning and normal operation to analyze the winding insulation and whether it can meet operational reliability standards. For online measurement, IEC 60034-27-2 [32] indicates that any frequency range, whether low (less than 3 MHz), high (3 to 30 MHz), very high (30 to 300 MHz), or ultra high (300 to 3000 MHz), can be used to detect PD; however, measurements of PDs in higher frequencies have greater advantages due to the smaller noise presence in that band [27,30]. On the other hand, high-frequency signals tend to be attenuated more easily, and thus are more effective at detecting PDs close to the excitation terminals.

3.5. Data Analysis and Pattern Recognition

The biggest challenge of online measurement is to analyze the characteristics and patterns of PD pulses to detect if they are present, and then identify the types of PD sources. In the literature, PD signals are analyzed through the pulse waveform in time and by Phase-Resolved Partial Discharge (PRPD) patterns, which are patterns formed by the pulse count in a given time window as a function of voltage (or charge) amplitude and the phase angle of PD pulse activity [13]. Figure 6 shows the pulse waveform and the PRPD pattern.

In Figure 6b, the signals collected by sensors have an amplitude at a given instant, which is associated with the phase angle of the supply voltage at the moment the PD occurs. To draw the PRPD, the amplitude and phase are divided into windows so that each pulse is classified according to its magnitude and phase; that is, each pulse will have its corresponding window. By obtaining the amplitudes and phases in a time interval, it is possible to perform the PD count for each window, thus obtaining the PRPD pattern. In addition, the sine wave used represents the phase-neutral voltage, used as a phase angle reference.

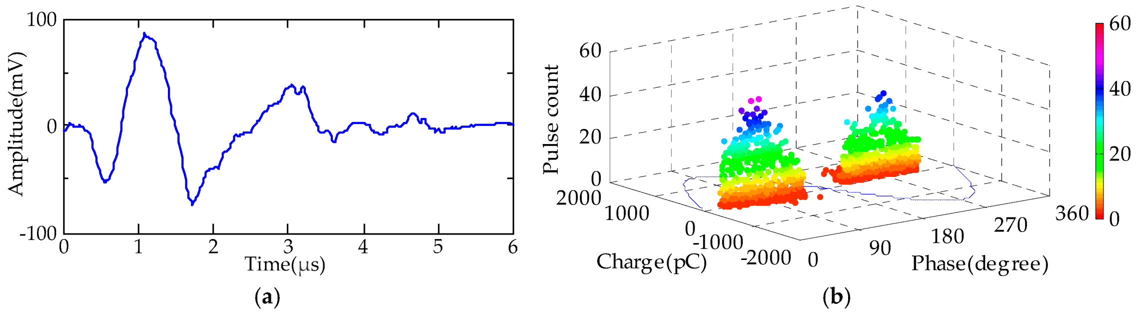

Figure 6. Data (**a**) waveform, (**b**) PRPD pattern [13].

The IEEE 1434 [20] presents three ways of analyzing the patterns of PDs that are quite widespread in the literature: the analysis of the PRPD pattern and the 2D pattern (pulse repetition rate as a function of amplitude), the utilization of the Time-Frequency (T-F) map, and Synchronous Three-Channel Multispectral Analyzer. In IEEE 1434 [20], examples of PD measurements on the stator coils of a typical machine are presented, with a voltage class of 13.8 kV.

3.5.1. Two-Dimensional Equivalent of the PRPD Pattern

This methodology was investigated in the laboratory through tests on coils that were removed from the stator core to apply artificial defects and analyze four groups of PDs, which are: internal discharges, slot discharges, end-winding discharges, and discharges from delamination of the main insulation from the inner conductor. For each type of PD, a PRPD pattern and a representation of the pulse rate by the PD amplitude were obtained, making it possible to analyze the geometric characteristics of the pulses in cycles of the PRPD pattern and the behavior of the 2D pattern, so that for each type of discharge, there will be a characteristic of its own [33].

Internal Discharges

The PD pattern presents symmetry in the half-cycles with low amplitude for the pulses and with rounded geometric characteristics [20]. Figure 7 shows the patterns.

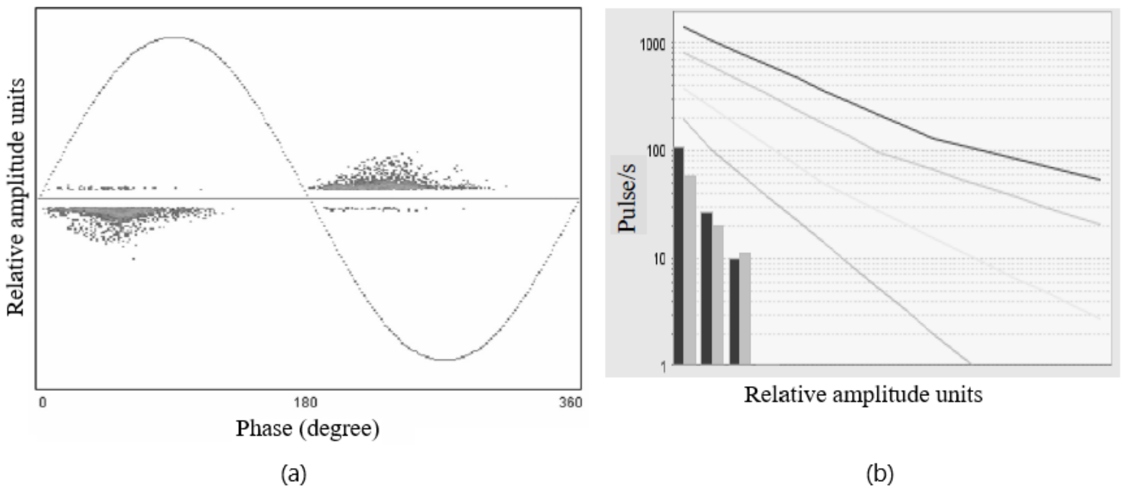

Figure 7. (**a**) PRPD pattern, (**b**) 2D equivalent [20,33].

Slot Discharges

The PD pattern presents asymmetry in the half-cycles with predominance for positive PD, the low amplitude for the pulses, and triangular geometric characteristics for the negative half-cycle [20], as shown in Figure 8.

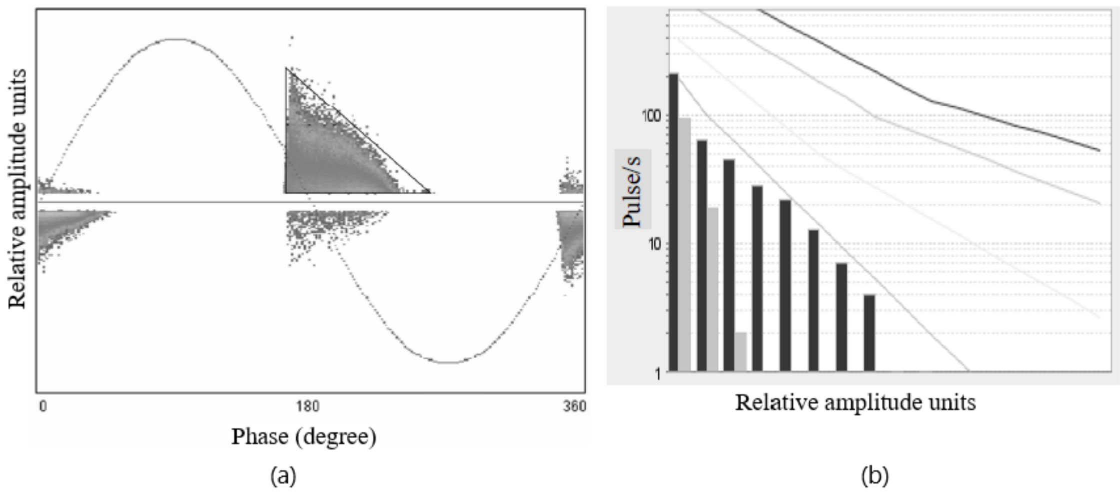

Figure 8. (**a**) PRPD pattern, (**b**) 2D equivalent [20,33].

External PD at the Stress Control Coating

The PD pattern presents asymmetry in the half-cycles, with a predominance for positive PD, a high amplitude for the pulses, and a more rounded geometric characteristic for the negative half-cycle [20], as shown in Figure 9.

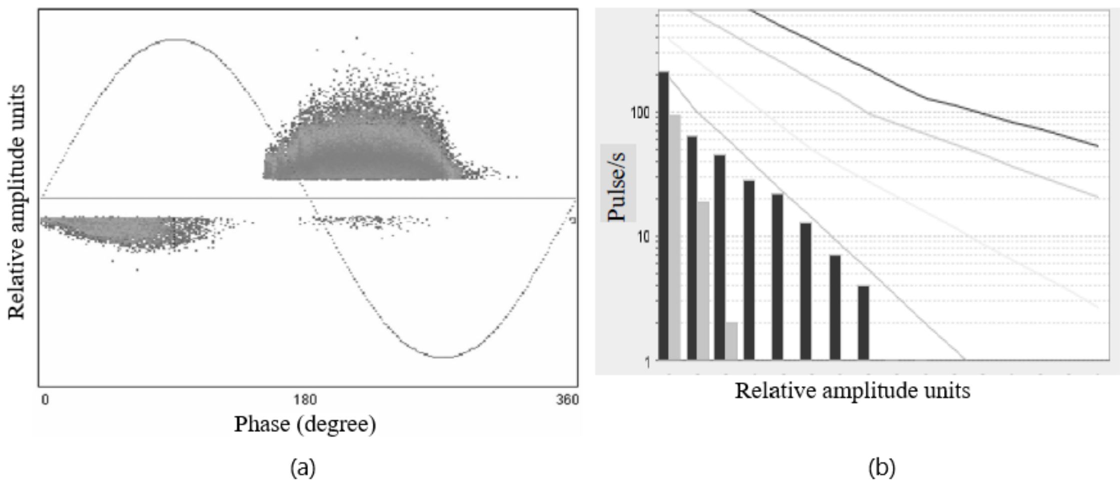

Figure 9. (**a**) PRPD pattern, (**b**) 2D equivalent [20,33].

Gap Discharges

The PD pattern presents symmetry in the half-cycles, with high amplitude for the pulses, and they are geometrically presented in the form of horizontal clouds [20,34]. Figure 10 shows the patterns.

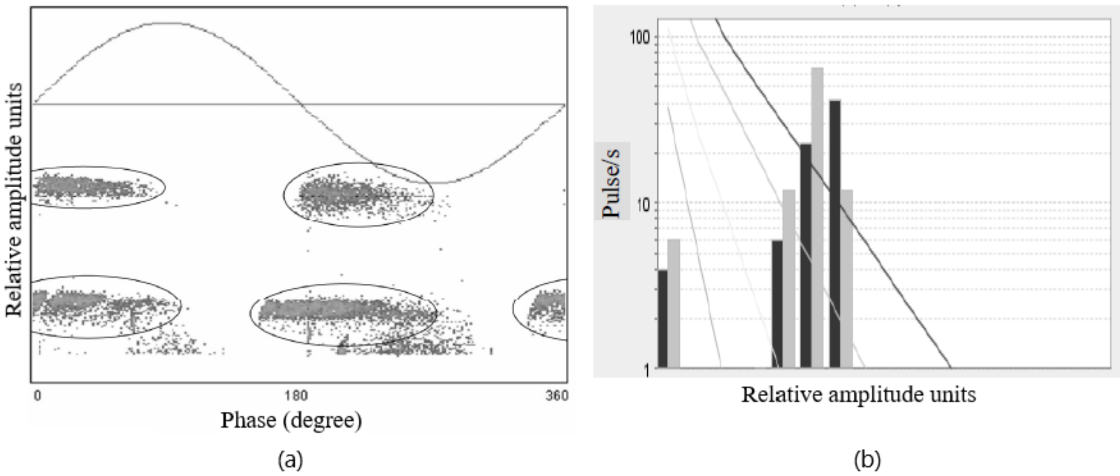

Figure 10. (**a**) PRPD pattern, (**b**) 2D equivalent [20,33].

Surface Discharges

The PD pattern presents asymmetry in the half-cycles, with high amplitude for negative PD pulses presenting geometrically in the form of vertical clouds between the angles of 30 and 40° [20], as shown in Figure 11.

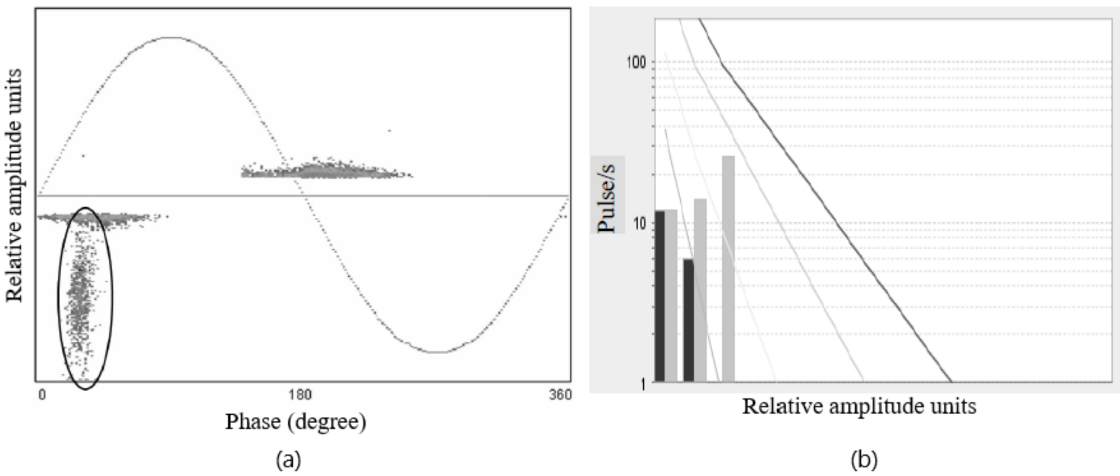

Figure 11. (**a**) PRPD pattern, (**b**) 2D equivalent [20,33].

Delamination

The PD pattern presents asymmetry in the half-cycles, with high amplitude for the negative PD pulses, and presents a more symmetrical geometry for the positive half-cycle. Figure 12 shows these patterns.

3.5.2. Time-Frequency Map (T-F)

In a real situation, where background noise and multiple PD sources are present, it is almost impossible to identify the different types of sources by coarsely analyzing the PRPD pattern. In these cases, the PD pulse is analyzed in terms of frequency and pulse duration time, since each type of signal will occupy a time-frequency band of its own. The T-F map allows separating the PD types and then analyzing the contents individually [35]. Figure 13 shows the T-F map and the individual patterns identified.

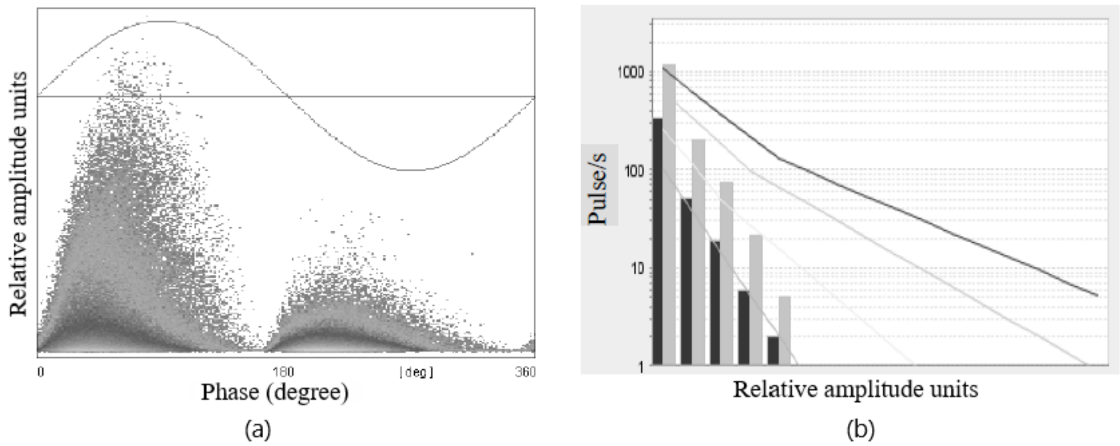

Figure 12. (**a**) PRPD pattern, (**b**) 2D equivalent [20,33].

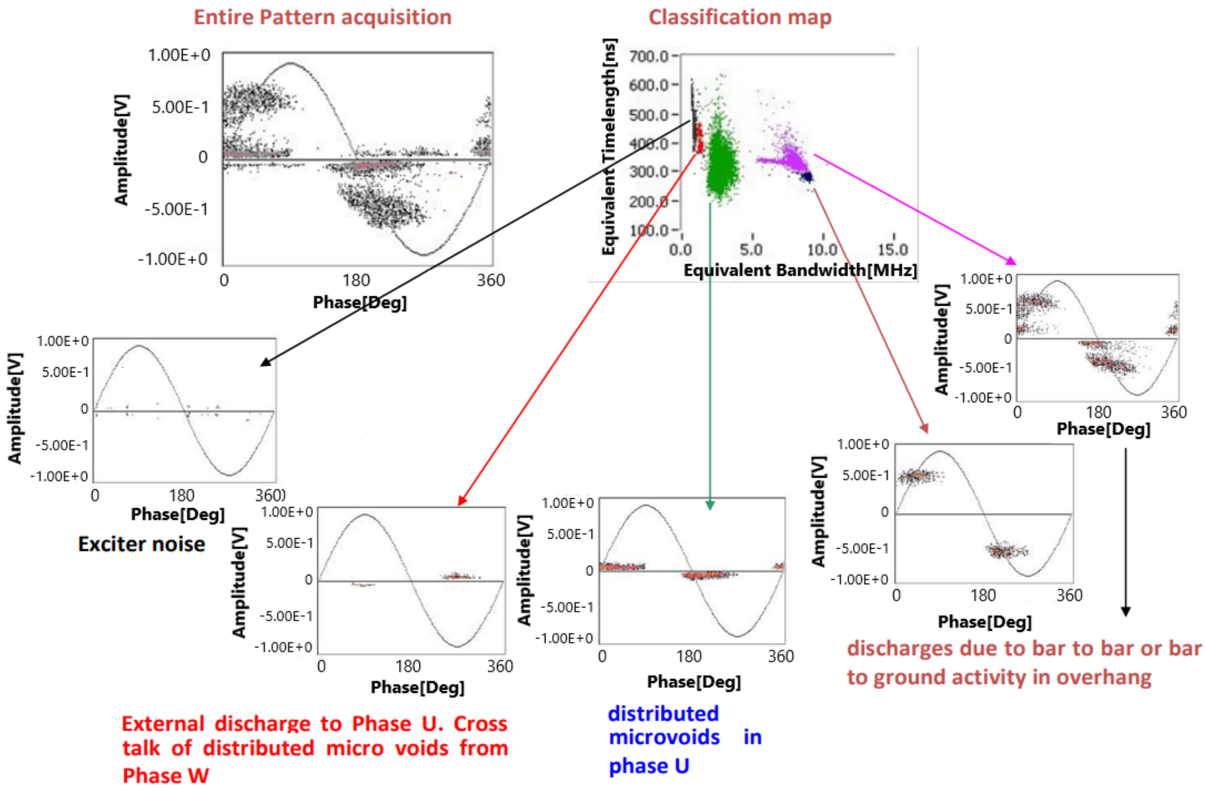

Figure 13. T-F map [20].

3.5.3. Synchronous Three-Channel Multispectral Analyzer

A very important factor in the monitoring of PDs that is rarely addressed in the literature corresponds to the capacitive and inductive coupling between adjacent coils, whether for single-layer windings, with one coil leg per slot, or double layers, with two coil legs per slot, or for coils of the same or different phases. In the case of adjacent coils of different phases, a PD pulse can propagate in more than one phase, making it difficult to identify in which phase the PD is occurring [29,36,37]. To circumvent this problem, the multispectral analyzer can detect the propagation of the PD pulse from a given source with different amplitudes in the three phases, forming vectors that give rise to a point, as shown in Figure 14. Several points form clouds that are defined as three-dimensional clusters. After that, the clusters are separated into PRPD patterns by phase or by type of sources to analyze the type of PD and in which phase it is located [38–40], as can be seen in Figure 15.

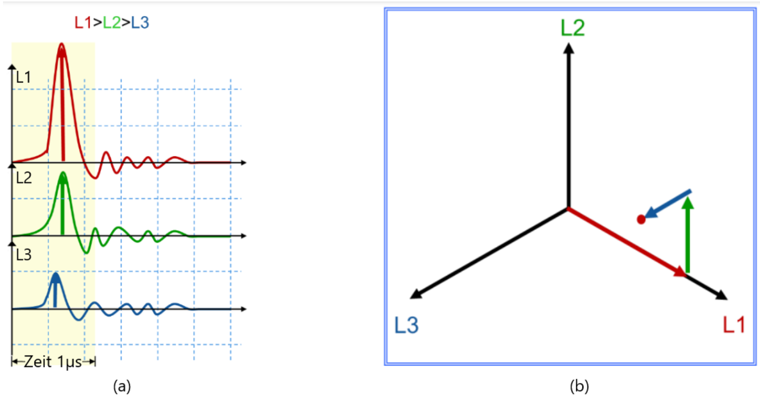

Figure 14. (**a**) Varying amplitudes in the three channels; (**b**) Vectors [38].

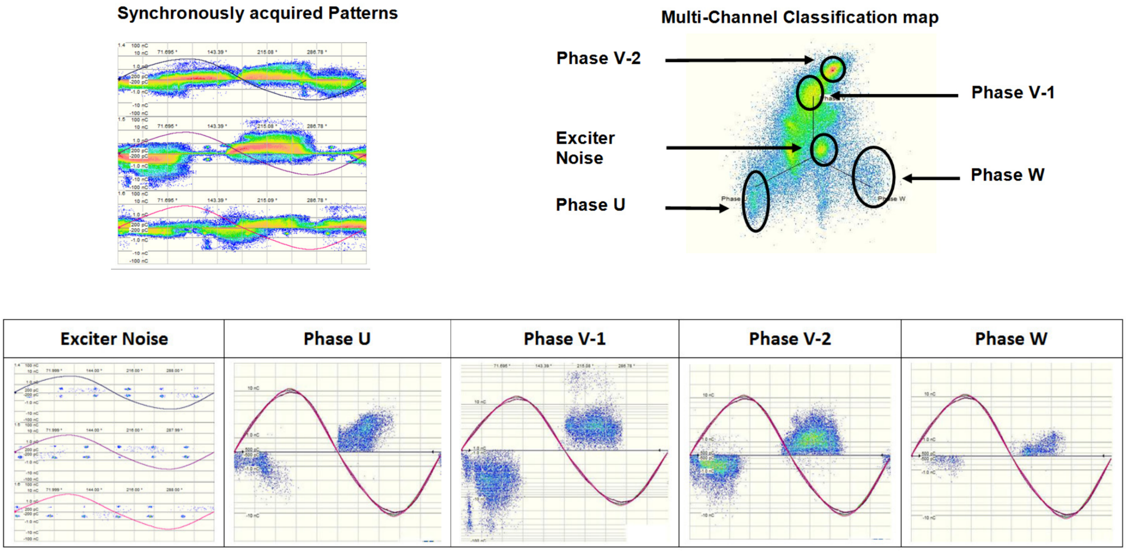

Figure 15. Patterns [20].

3.5.4. Statistical Analysis of Data

Statistical analysis is a very useful tool when you have an extensive database of PD measurements that encompass machines with different characteristics, such as cooling types and voltage classes. With this, it is possible to establish PD levels according to the characteristics of the machines in order to facilitate the identification of problems. A prevalent method in the literature corresponds to the use of the cumulative probability of failures related to the maximum discharge amplitude (Q_m), given in [41]. Figure 16 shows a graph of measurements of PDs in the high-frequency range for hydrogen cooled machines of different voltage classes, with the vertical axis represented by Q_m and the horizontal axis by the cumulative probability of failure.

In [41], based on the authors' experience, the 90% level is used as an alarm to indicate high PD activity. Thus, the Q_m measured by each sensor is classified according to the cumulative probability, with the limits defined according to some characteristics of the machines.

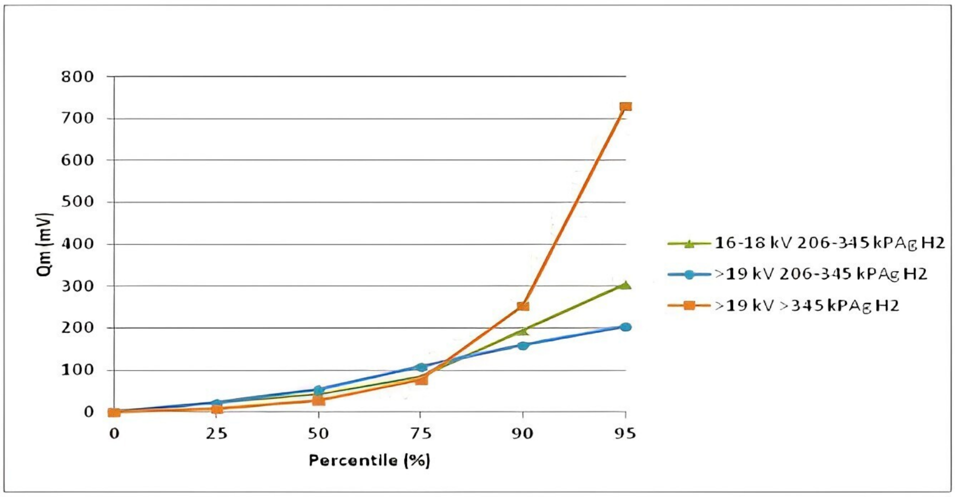

Figure 16. Curves for respective voltage classes [41].

3.6. Acceptance Limits Based on PD Measurements

Monitoring the actual state of the insulation of a machine winding requires the definition of compatible PD levels for each type of machine so that the sources of PDs can be reliably identified. The main reason for this is because PD acts differently in each machine, not being able to reliably establish a predefined threshold of PD without first analyzing the machine particularities. In the literature, thresholds are generally defined in voltage or charge units and are based on standards, where the circumstances in which the measurements were obtained are not explicit.

Some studies use the maximum amplitude of 1000 pC as a reference to indicate PD activity in medium voltage machines, this threshold being based on international standards [42]. To verify this value, in [42], tests were realized in a hydro generator, where voltages of 7, 9, 10.5, and 11 kV were applied to the machine terminal, and PDs were measured. It was found that with the increase in the voltage level, the measured charge also increases, being greater than 1000 pC, which is the amplitude taken as a reference. For the voltage of 7 kV, the discharges in phase A were measured with an amplitude of 3800 pC, while for the voltage of 11 kV, a charge of 6500 pC was measured. The study recommends a visual inspection to analyze the condition of the winding, analysis of electrical parameters, and insulation of the stator coil, in addition to the realization of annual measurements to ensure more reliability in diagnosing the status of the machine.

In [43], PD levels were defined for stator windings of industrial motors with voltage classes from 10 kV to 15 kV, without providing information to explain how and under what circumstances these levels should be applied [44]. Table 1 shows the levels defined in [43].

Table 1. PD levels [43].

Condition Assessment	Peak PD Level (nC)
Excellent	<2
Good	2 to 4
Average	4 to 10
Still acceptable	10 to 15
Inspection recommended	15 to 25
Unreliable	>25

In [45], a statistical analysis of the PD data was presented through tables of distribution of maximum discharge amplitude, showing that for machines with different voltage classes, cooling models, and types of sensor of PD, the results were different. Therefore, it is necessary to be careful with the defined thresholds, as the hasty choice of a limit may lead to faulty assessments.

In the offline tests of [28,44], PD pulses were applied in different regions of the stator winding of a 15 kV turbo generator and a 12.5 kV induction motor, respectively. For all locations, the injected pulses were measured with different magnitudes, depending on the coupler configuration used. It was found that the lower the frequency range, the better the measurement sensitivity of apparent charge. It was also observed that the pulse peak measured by the sensor is more attenuated as the injected pulse is applied further away from the measurement point. Furthermore, the study of [28] draws attention to the effect of the inductive and capacitive couplings between adjacent coils, where the pulse propagates differently for low- and high-frequency modes (or slow and fast modes). Figure 17 presents a schematic of the path taken by the injected pulse for the high- and low-frequency components of a typical winding.

Given the above, it is possible to identify some factors that directly influence the measurements of PDs and the definition of thresholds, as follows: machine voltage class, type of cooling, type of sensor used for data collection, selected frequency band, and place of occurrence of the discharge and coupling between adjacent coils. All these factors must be taken into account to define the guidelines that will be used to identify PD activity so that a reliable analysis is available for each type of machine. To define an acceptance limit based on PD measurements, it is also essential to have a large amount of data from similar machines operating under similar conditions of power, temperature, humidity, etc., allowing an analysis to be realized with significant statistical information to establish a reliable criterion.

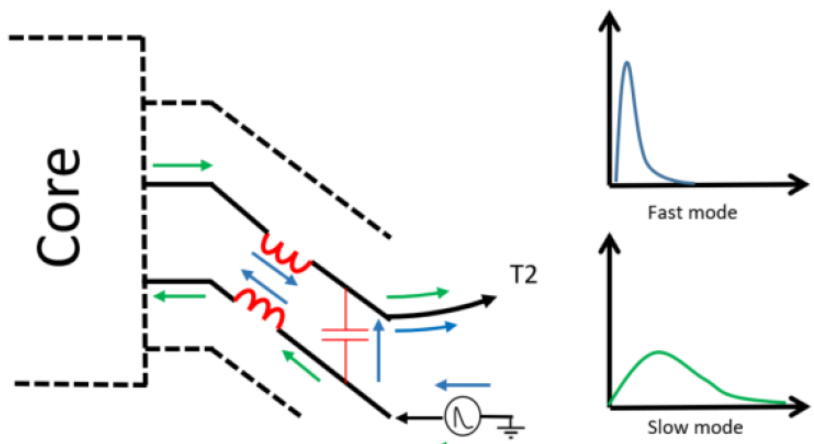

Figure 17. Capacitive and inductive coupling between bus [28].

4. Review of Commercial Equipment

Commercial equipment for PD detection appeared initially in the 1970s. Since then, the methods have been evolving and adapting to the needs identified by several customers. At the turn of the millennium, there was rapid progress, with automated systems emerging incorporating digital signal processing techniques. Recently, the demand for online methods that allow storage of PD data and detection of incipient failures using virtual instrumentation and Artificial Intelligence (AI) has ensured the continuous development of these technologies.

Methods for detecting PD signals are also evolving. The established methods are: Neutral HFCT Coupling (NCT), Neutral Capacitor Coupling (NCC), HV Terminal HFCT Coupling (HVCT) and HV Terminal Capacitor Coupling (HVCC) [13]. These methods have been used individually or together by several manufacturers for over 50 years for PD-based detection and diagnosis of large machines.

Over the years, the NCT method, although reliable, has become outdated, as it only detects severe PD. The NCC method inherits the reliability of the NCT, but delivers a result with better sensitivity. However, NC methods have limitations regarding low SNR. On the other hand, the HV methods are more modern, allow differential and directional measurements, and also allow the use of smaller and standardized coupling elements.

Although several manufacturers use the same acronyms, there are important differences between their technologies, especially concerning signal interpretation and classification techniques.

The vast majority of commercial methods for detecting PD in large machines use one of two coupling elements (called sensors by some manufacturers): a High-Frequency Current Transformer (HFCT) or a Coupling Capacitor (CC). These elements filter out the low-frequency components that—in theory—are not part of the PD signal to be analyzed. Figure 18 shows some of these devices.

Figure 18. Photograph of some (**a**) HFCTs [46] and (**b**) coupling capacitors [47] used for PD system.

The choice of this coupling element directly impacts the frequency range used by the detection method. In the 1980s and 1990s, after several studies, the Ontario Hydro company defined the value of coupling capacitors as 80 pF. This choice results in the rejection of signals with frequencies below 40 MHz. Although effective in denoising, this choice results in low sensitivity of detection of PD events with low frequencies, mainly below 30 MHz. However, these PD events do occur and are related to important impairments in the equipment. Another important feature is the vertical resolution, which in the basic mode of this device is 4 bits. This is relatively low when compared to other devices.

The choice of capacitors in the nF range (two to three orders of magnitude greater than those defined by Ontario Hydro) is used by other manufacturers, in which the method is based on the detection of low-frequency events (tens of kHz up to 20 or 30 MHz). Since these lower frequencies often contain high noise levels, these devices employ denoising methods using some form of digital signal processing. Table 2 presents characteristics of some commercial systems for detecting PDs. Some equipment, such as the MPD 800 and MONTESTO by OMICRON, uses 2 nF coupling capacitors but is also able to normally measure PD events on machines with 80 pF coupling capacitors already installed. The MPD800 is a digital, portable, modular PD monitoring system that includes an optical communication system and allows simultaneous measurements of two or (using an additional module) three phases.

Table 2. Resume of characteristics of some commercial PD online measurement systems for large generators adapted from [13].

Detection Point	Vender	Product	Detection Method	Sensor	Frequency Range
Neutral	OMICRON	MPD 800 [48]	NCT + HVCC	1 HFCT + 1 2 nF CC	6 kHz~35 MHz
HV terminal	IRIS Power	TGA-B [49]	HVCC HVCC	6 80 pF CC 6 1 nF/2 nF CC	40 MHz~350 MHz 2 MHz~350 MHz
		PDA-IV [50]	HVCC	6 80 pF CC	0.1 MHz~350 MHz
	Doble	doblePRIME PD-Guard [51]	HVCT + NCT	4 HFCT	50 kHz~100 MHz
	OMICRON	MONGEMO [52] MONTESTO 200 [53]	HVCC HVCC	3 80 pF/2.2 nF CC 3 1 nF/2 nF CC	16 kHz~30 MHz 16 kHz~30 MHz
	HPVD	HVPD Kronos Permanent Monitor [54]	HVCC HVCT	3 CC 3 HFCT	100 kHz~50 MHz
	TECHIMP- Altanova Group	PD Hub [55]	HVCC HVCT	3 CC 3 HFCT	16 kHz~30 MHz
	Megger	ICMmonitor [56]	HVCC	3 CC	2 MHz~20 MHz
	CEPEL	IMA-DP [57]	NA	NA	3 MHz~30 MHz
	Amperis	PXDP-II [58]	HVCC	2 CC/HFCT	300 kHz~70 MHz
	Sparks Instruments	Escort TMS-6141 [59]	HVCC + NCC	4 CC	40 kHz~300 MHz
	PDS	PDSimply [60]	HVCC	6 80 pF/1000 pFCC	150 MHz~1.2 GHz
Neutral/ HV terminal/ RTD	Dynamics Ratings	DRPD-15 [61]	NCC/NCT/ HVCT/HVCC/ RTDs	CCs/ HFCTs/ RTDs	1 MHz~20 MHz

In many markets, two of the most common kinds of commercial equipment installed to monitor PD are the IRIS Power TGA-B and OMICROM MPD 800. The photographs and characteristics of both devices are shown in Figure 19 and Table 3, respectively.

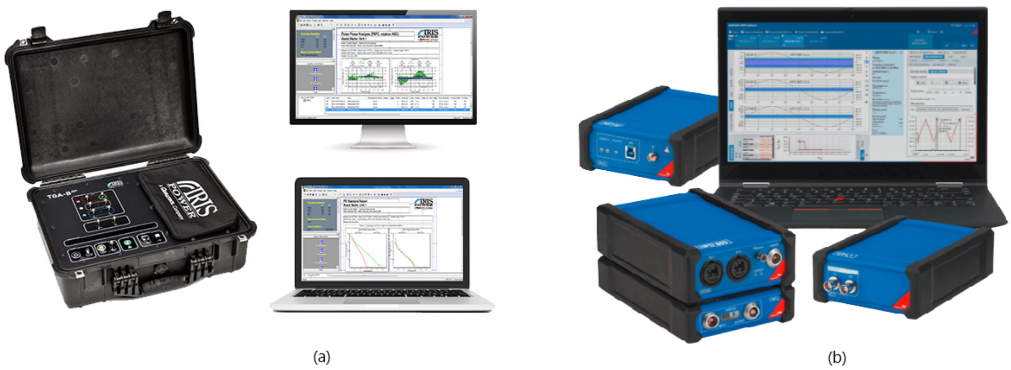

Figure 19. Photograph of commercially available commercial equipment taken in the year 2022 by their manufacturers: (**a**) the TGA-B of IRIS Power [49] and (**b**) the MPD 800 of OMICRON [48].

To overcome the problem of low sensitivity for PD events at low frequencies, IRIS Power offers optional accessories, including couplers for different voltage levels. The MPD800 also has optional accessories such as VHF and UHF sensors, a pulse generator, a high-frequency current transformer, coupling capacitors for different voltage levels, a balanced bridge, a charge calibrator, etc.

The MONTESTO 200 model allows simultaneous three-phase measurements (without any additional module). It has the same technical versatility as the MPD 800, but it incorporates an additional feature, which is the possibility of being used as a continuous monitoring instrument. With internal memory capacity, it can be programmed and left connected, for example, to a generator for a continuous data acquisition campaign for a long period, such as a month. In addition to traditional auxiliary power, it can also be powered by a 12 V automotive battery, which allows its use in remote locations.

Table 3. Characteristics of the most used commercial equipment.

Description	**TGA-B**	**MPD 800**
Frequency range	40 MHz–350 MHz 0.1 MHz–350 MHz (with accessories)	6 kHz–35 MHz
Multiphase acquisition	Sequential	Simultaneous and synchronous
Maximum amplitude peak	34 V	80 V
Battery operated	Yes	Yes
Optical fiber communication	NA	Yes, 2 × LC
Operating Temperature	−15 °C to 45 °C	−20 °C to 55 °C
Relative humidity	to 95% uncondensed	55 to 95% uncondensed
Dimensions	410 mm × 310 mm × 210 mm (W × D × H)	119 mm × 55 mm × 190 mm
Weight	10 kg	0.87 kg

Unlike the equipment shown so far, the DRPD-15—shown in Figure 20—presents an additional option that is based on the detection of RF signals transmitted through the air using the cables of Resistance Temperature Detectors (RTDs). The high-frequency components caused by PDs generate electromagnetic pulses that can be absorbed by antennas inside the machine. Capacitive couplers and HFCTs can also be used with the DRPD-15 to detect PDs. More details regarding measurements using RTDs are presented in Section 5.4.

Figure 20. Portable equipment model DRPD-15 of Dynamics Ratings [61].

Since the 2000s, a group of researchers of the Electric Energy Research Center (CEPEL, from Portuguese *Centro de Pesquisas de Energia Elétrica*) has been developing a system for the diagnosis of electrical equipment called Discharge Monitoring and Analysis Partial (IMA-DP, from Portuguese *Instrumentação para Monitoramento e Análise de Descargas Parciais*). The project was awarded in the "Energy" category of the Global Engineering Impact Awards—2018 technological innovation contest [62].

The IMA-DP is a modular system that can be adapted to the applications, and to the electrical equipment monitored, especially rotating machines. The IMA-DP operates using non-proprietary hardware that collects the PD signals at high frequency. This aspect provides some flexibility in defining the arrangement adopted, but on the other hand, it is not a fully integrated hardware and software system. The IMA-DP system (software) allows working with an acquisition rate of up to 125 MHz and a resolution of up to 12 bits. The acquisition can be simultaneous in all three phases, or individually per phase or measurement point.

5. State of the Art in Measurement and Analysis of PDs.

In the literature, the recognition of PD patterns is based on the comparison with patterns established in technical documents such as IEEE 1434 [20], and in statistical or machine learning techniques. However, for rotating machines, there is still a preference for the first approach, making the analysis somewhat limited and unreliable, as each machine has a different design (voltage class, type of cooling, etc.) and works in specific environments. Therefore, it would be most convenient to analyze the PD history of each asset, creating taylor-made decision rules [42,44,45,63–65]. In addition, PDs are measured with different magnitudes, depending on the applied filter settings as well as the frequency response of sensors. Other factors that can also influence the measurements are the distance of the couplers and the cabling used because, in some cases, the signals are distorted or attenuated [44,45]. Establishing absolute intervention limits for all machines may not be as feasible. It is possible to improve this threshold criterion by analyzing the relative values of each machine over time.

Due to the numerous open questions in the study of PDs, the topic is widely discussed in the academic literature. In this section, references on the state of the art in the study of PDs found during the literature review are discussed.

Methodologies for analyzing data collected by capacitive sensors, and current transformers, among others, based on comparison with standards and machine learning will be discussed. In addition, approaches related to the influence of the drive system on the detection of PDs and the location of PDs will be presented.

5.1. Analysis of Data Collected by Capacitive Sensors

This subsection will review methods for detecting PD based on data collected by capacitive sensors. We will first review methods that use statistical analysis and comparison with existing PD standards. For that, the references will be organized according to the capacitor installation schemes described in Section 3.3.1. Then, we will review methods based on machine learning.

5.1.1. Comparison with Standards and Statistical Analysis

Simple Method

In [35,66–68], data were collected using only one sensor per phase at the terminals; that is, in the simple form.

The methodology of [66] presents a statistical approach to analyzing the intensity of PD in machines. Identification is carried out when the PD intensity alarm level is exceeded. PRPD patterns are used to analyze the progression of PD activity. In addition, [66] proposes an autonomous system that generates analysis reports continuously.

In [35] the T-F map approach was used to discriminate between PDs in the grading region and the discharges in the slot region. A statistical analysis of the voltage pulse magnitude and repetition rate data is performed to identify PDs in a 30 MVA synchronous generator.

The multispectral analysis of three synchronous channels is used in [67] to obtain the PRPD patterns from the three-dimensional clusters and identify the types of PDs.

In [68], the collection of data from the assets was performed using capacitive couplers of 500 pF, and the PDs data were separated from the noise using a heat map of a 2D pattern formed by the peak and frequency of the PD pulses. The identification of PD patterns was performed by separating the PD pulses based on their frequency content.

Directional Method

In [41,64,69–71], the online monitoring of PDs was performed using two capacitive sensors per phase. In the studies [41,64,69,71] sensors of 80 pF were used, and in [70], it was not specified.

In [41,64,69–71] a PRPD pattern is used to identify PD activity in generators with different types of cooling. In [41,64], PRPD patterns are presented for measurements of capacitive sensors and antennas, in addition to showing the effect of the type of cooling on the PD amplitude. Statistical analysis is presented to detect the cumulative failure probability by analyzing the maximum PD amplitude for machines with different voltage and cooling classes. With the analysis, it is possible to verify that in some cases, depending on the design of the machine, the sensors have similar sensitivity, and in other cases, one of the sensors stands out concerning the other. However, it must be taken into account that the PD detection using an antenna is an intrusive method, as it is located inside the stator. In [69,70], the PD data of a 21 kV generator and turbo generators are analyzed by locating the PD pulses concerning the phase angle.

In [71] the data of a gas turbine generator were analyzed using heat maps that present the pulse amplitude and the PDs frequency. The methodology was useful for signal filtering and discrimination of the PD patterns. The different types of PD and noise pulses were separated based on their frequency content.

Differential Method

The differential mode was used in [72], where the monitoring of generating units at UHE Balbina was described. Data were collected by 80 pF capacitive sensors and analyzed by pulse repetition rate by PD amplitude. It was observed that the generating unit number 3 presented a high level of PD activity with a high Normal Quantized Number (NQN) and maximum amplitude (Q_m), which exceeded the predefined limits. After visual inspection, degradation was identified in the grading region, which showed that the method was successful in using PDs to identify problems in the generator.

5.1.2. Machine Learning

The literature still presents few machine learning applications to detect and identify sources of PDs in rotating electrical machines. Of the few references found on machine learning, there is a predominance of techniques that use clustering algorithms to identify data clusters and neural networks to classify images of PD patterns.

In [73,74] experiments performed in the laboratory on small motors with their own insulation characteristics, different from those of large machines, were presented. In [73], four artificial defects were applied to the winding of eight motors. The PD signal was collected using a capacitive coupler, and the detection was based on magnitudes and the number of PD pulses. The signals obtained from each defect were mixed, creating a mixed signal, which together with the individual signals was used in analysis to determine statistical characteristics, correlation functions, and width parameter of the Cumulative Energy (CE) of PDs. After extracting the characteristics of the CE signal, the K-means algorithm was trained to separate the individual and mixed PD signals from multiple defects, in some cases reaching classification accuracy of 91.9% for individual signals and 92.7% for simultaneous defects, proving to be robust to classify PDs. In [74], five artificial defects were applied in the winding of 10 motors. The classification of PD data was based on CE signals using the K-means algorithm. In addition, the failure probability and isolation severity estimation were based on the Weibull distribution.

In the studies of [75–78], data from hydro generators were analyzed using the IMA-DP produced by the CEPEL [79,80]. In [75–77] the PRPD patterns obtained from the IMA-DP are analyzed using images. The PD content in the images is based on clouds (concentration of points) so that contours are defined for regions of higher density. After defining the region, histograms showing patterns from different sources of PD were calculated, and then artificial neural networks were utilized to classify the data. Overall classification accuracy rates for [75] were greater than 88% for all PD sources considered. In [76], the classification accuracies were greater than 87% for all PD sources. In [77], the recognition rate was higher than 94%. In [78], after preprocessing of the data obtained from the IMA-DP and analysis of the PD pulse maximum amplitude, the data were labeled using clusters and then a random forest algorithm was trained to classify the data. Of eight trained random forest models, five achieved classification accuracy above 99%.

5.2. Analysis of Data Collected by HFCT, Antennas, and Others

This subsection will explore data analysis methodologies for detecting PDs through standards comparison and machine learning, using data collected by HFCTs, antennas, and other sensors.

5.2.1. Comparison with Standards and Statistical Analysis

In [22] an online monitoring system for electric motors was presented. In that system, PD data were collected through current transformers allocated to each phase. Data analysis used a combination of three features, which were the peak level of PDs, number of pulses of PDs, and PD activity, which were associated with the degradation of the conductor insulation. The increase in peak levels and PD activity were used as indicators of the occurrence of failures. The PRPD pattern was also used to identify the types of PD sources, and a visual inspection was performed to confirm the diagnosis.

In the study [81], three data acquisition methods were used, based on capacitive sensors and current transformers, as well as denoising filters for each method. The best result was obtained using HFCT sensors and a Wavelet filter for background denoising. The results were analyzed through three-dimensional PRPD patterns that gave rise to 2D patterns per phase that were compared to IEC 60034-27 [18] standards.

In [82] a web application implemented by HydroQuebec to monitor its assets was presented. This application, called MIDA, centralizes the diagnostic data of the machines. MIDA data were used to identify symptoms of physical degradation states of the stator winding using a method defined as Failure Mechanism and Symptom Analysis (FMSA). The FMSA has three main stages of analysis, which are defined as the root cause (what caused the insulation degradation), failure mechanisms (winding abnormality indicator), and failure modes (failures associated with the winding). An example is the contamination of the grading layer (root cause), which leads to an increase in the electric field concentration and, consequently, an increase in PD activity in that region (failure mechanism), resulting in the degradation of the insulation in the grading region (failure mode). An important analysis that the study presents is the transition from one type of PD to another in a given period, which could cause the operator to make the wrong decision before the failure occurs. The identification of this PD transition period is extremely important when it comes to determining the root cause, as it makes it possible to identify which PD occurred first, then associate their characteristics with the root cause, and also understand how they are related to the activity that occurred later.

5.2.2. Machine Learning

In [83] an unsupervised methodology was used in which data were collected from current transformers. The data of the PRPD pattern were projected in two principal components, using the Principal Component Analysis (PCA) method to identify clusters of surface, internal, and noise discharges. The clusters generated by noise signals were then rejected. In addition, a methodology based on the shape of the signal pulse and the distribution of the risk rate was also presented, both of which are utilized for the separation and recognition of the PD signal. To identify the sources of PD, the authors used fuzzy logic.

In the study [23], PD data were collected through current transformers allocated to the grounding of the machines' neutral closure. First, the data were filtered using the Adaptive Local Iterative Filter (ALIF) method, which is a time-frequency signal decomposition methodology based on a partial differential equation model. After applying the ALIF method, the permutation entropy was calculated, which is based on the Shannon entropy that estimates the significant information in data. Then, the Support Vector Machine (SVM) algorithm was applied to distinguish different sources of PD. The algorithm achieved 96% classification accuracy.

In [84] four supervised learning techniques were used to classify four sources of PDs from PRPD patterns. The techniques used consisted of functional based techniques (Logistic Regression (LR), SVM, Multilayer Perceptron (MLP)), probabilistic techniques, decision trees, and nearest neighbor. From a universe of 351 examples, 246 were used for training and 105 for testing. Accuracy and area under the curve were used to determine the best PD classifier. The SVM and MLP obtained an overall classification accuracy of 99.1%.

The methodology presented in [85] combines the knowledge of a PD specialist with the use of artificial neural networks to classify a PD database. First, the specialist, using his experience in 2D PD equivalent analysis (discharge rate x amplitude), selected 100 PD data from a universe of 33.222 samples, for which he already knew the type of PD source based on the symmetry characteristics of the amplitudes of the positive and negative discharges. Then, the selected data were converted into input vectors of a neural network to be trained, since the authors claim that training a neural network with certain data from each PD class is more powerful than selecting a large dataset. After each training step, the data are projected into a 2D latent space, making it possible to visualize clusters of PD sources and facilitating the location of low-density regions. These regions may point to the need for additional data to be selected and labeled by the expert to improve the classification. Then, statistics of the discharge rate as a function of the amplitude of the classes are calculated to define the behavior of each PD class.

The studies presented in [86–88] used MIDA data from the company HydroQuebec and were based on Autoencoders, which are artificial neural networks that learn efficient representations of input data, a process defined as encoding, without the need for supervision. These neural networks are able to randomly generate new data very similar to the training data, a process defined as decoding [89]. The version used in the studies is the Variational Autoencoder (VAE), which is a probabilistic and generative autoencoder with the ability to generate new instances that seem to have been sampled from the training set [89]. Figure 21 shows the structure that was used in the methodologies, with $\boldsymbol{X}$ being the inputs set, $\boldsymbol{\mu}$ the average vector, $\boldsymbol{\sigma}$ the standard deviation vector, $\boldsymbol{Z}$ the latent vector, with $\boldsymbol{Z} \in \mathcal{R}^2$ having its elements calculated by Equation (1) and $\hat{\boldsymbol{X}}$ as the outputs (reconstructed data).

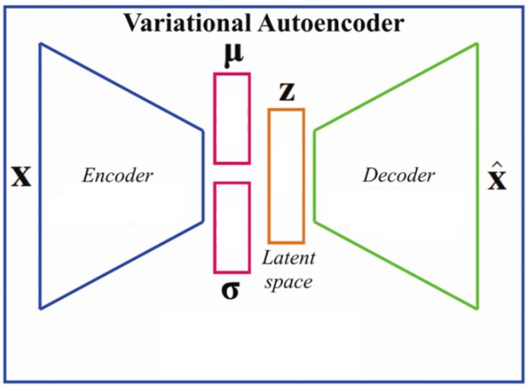

Figure 21. Variational Autoencoder, adapted from [87].

The latent vector, given by Equation (1), is a coded representation of the characteristics of the input data, which in this case is the PDs. In Equation (1), ϵ is a random variable with normal distribution.

$$\begin{aligned} z_i &= \mu_i + \sigma_i.\epsilon \\ \epsilon &\sim \mathcal{N}(0,1) \end{aligned} \tag{1}$$

In [86] the PD data were coded and displayed in 2D space using the latent vector, allowing an expert to visualize the data distribution, find the class boundaries, and then label each cluster. The data and labels are then used to train a neural network to classify the types of PDs. Figure 22 shows the structure used in [86], being presented in the data visualization in two components of the latent vector defined as z_1 and z_2, where each PD class is represented by different colors. The overall accuracy of the classification obtained by the model was 65%. However, for some sources of PDs, this accuracy does not exceed 35%. In [87], the methodology presented was divided into two main stages, which are unsupervised and supervised learning. The unsupervised step was responsible for training the VAE to obtain characteristics of the input data and visualize them in the 2D latent space. The supervised step consists of training the structure (encoder–classifier) to detect anomalies. Furthermore, in supervised training, a small amount of labeled data were used to obtain better data segmentation and less cluster overlap. Visualization of the results in 2D space after classification allowed the easy identification of clusters of PDs, enabling the analysis of an expert to evaluate the performance of the given diagnosis. In [88], initially, the PD data were filtered based on the minimum discharge rate to eliminate data with low PD levels. The filtered data were then used as encoder inputs and were also projected in a 2D space, allowing visualization of the data distribution, allowing us to find the limits of classes and conflict zones (the region where the classes overlap). Finally, 10 classifiers were used, so that the output label was defined as the average of the ten, which must be greater than a pre-defined threshold. The overall classification accuracy obtained by the method was 44.1%.

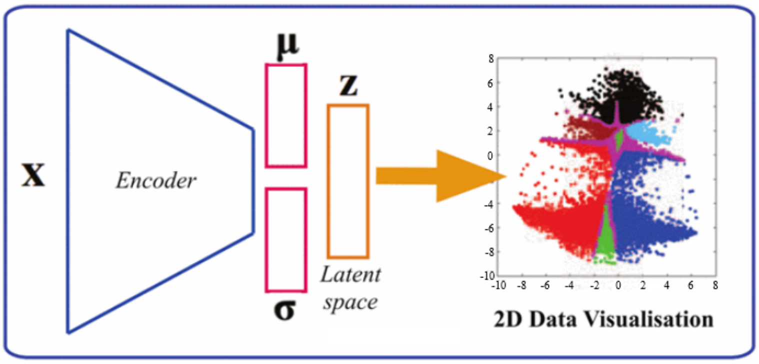

Figure 22. Data visualization [87].

5.3. Influence of the Drive System on the PD Reading

In the literature, there are still few studies that consider the influence of machine drives by frequency inverters in PD monitoring. This type of study is important because the drive using PWM is becoming common in petrochemical and industrial facilities. During the operation of a motor, due to the commutation process using PWM, some voltage pulses can be confused with PD activities if the monitoring system is not calibrated considering this factor and if it does not have additional filtering with an adjusted frequency band [90]. In addition, it should also be taken into account that the voltage harmonics caused by inverters may amplify PD signals, as shown in [91], where it was found that the greater the Total Harmonic Distortion (THD), the greater the number of discharge pulses and, in some cases, the greater the PD amplitude. Another factor that influences the PD activity is the applied supply voltage waveform, since from [92], it is possible to verify that three different PD patterns are generated for three supply waveforms coming from inverters of two levels, five levels, and sinusoidal voltage. With the use of inverters, the PD cycles change and the PD amplitude also changes.

An important factor that may result in a false diagnosis of PDs in variable speed motors is the identification of the fundamental electrical frequency applied to the machine. This information is crucial for identifying the PDs in the corresponding cycles of the sine wave shown in Figure 6b, since for different speeds of a machine, voltage signals of different frequencies are applied.

Given the discussion above, some challenges must be addressed, which are the separation of the PD signal from the switching noise, obtaining the voltage waveform at the fundamental frequency to assist in the formation of the PRPD pattern and how to recognize fundamental frequencies of the input voltage for different motor speeds [93,94].

In [95], the challenges are addressed. The study uses capacitive sensors of 80 pF to read the data; a voltage divider, as shown in Figure 23, to provide the synchronization signal at the fundamental frequency; plus additional filtering to eliminate pulses caused by switching. Data analysis was performed via PRPD pattern analysis to identify PD activity in 7.2 kV, 4.1 kV, and 3 kV motors operating at frequencies of 100, 50, and 50/60 Hz, respectively.

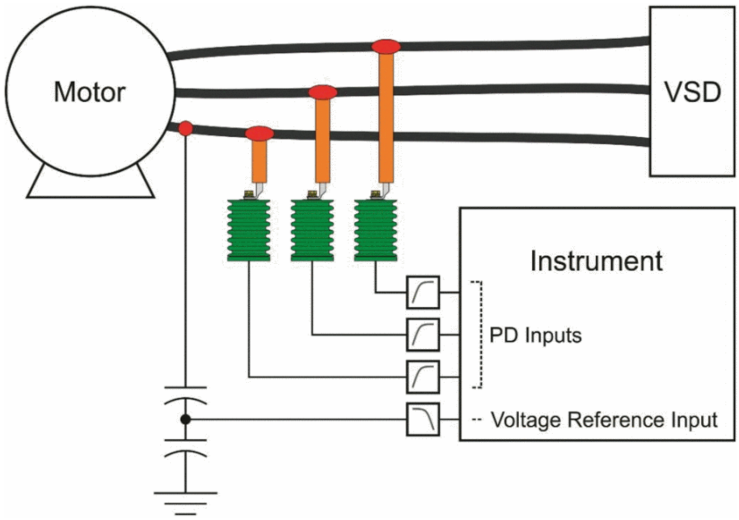

Figure 23. Structure of the PD measurement system [95].

In [96], an analysis of surface PD in the semiconductive region of the winding of 6 kV machines driven by frequency inverters is presented. The analysis was based on PRPDs patterns and ozone monitoring. For the PRPD with cycles based on the operating frequency of 60 Hz, there was great activity of negative PD between 0 and 90° and positive PD between 180 and 270°, with positive PD amplitude greater than that of negative PD, characterizing PD in the semiconductive region. Ozone monitoring was performed via a MOSFET sensor, which identified a high increase in ozone concentration, characteristic of surface PD.

5.4. Methods for Locating PDs

Methods for estimating the location of PDs in the stator windings of rotating electrical machines are rarely presented in the literature due to the high level of complexity. In this subsection, studies that use RTDs and software to locate PDs will be described.

5.4.1. Use of RTDs

RTDs are installed in the stator slots of large electric motors and generators in order to monitor the temperature rise. Some studies use the RTDs present in some machines as a complementary way to help with the identification of areas where PDs occur. The proposal is motivated by the fact that the coupling capacitors installed in the line terminal of a machine have a detection zone of 10 to 15% of the total winding, which can be improved with the use of RTDs [97]. For this application, the RTD works as an antenna for propagating PD pulses. This is possible because as the PD pulse propagates in the RTD region, the energy of the PD is coupled to the RTD or to the RTD conductor [98]. Figure 24 presents the

RTD allocation scheme in the stator slot of a typical machine to indicate the way the pulse propagates.

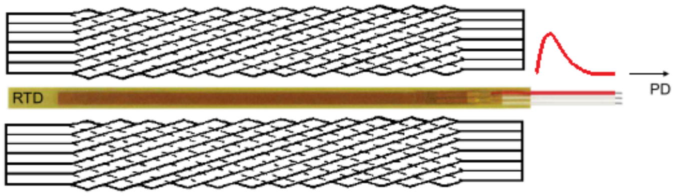

Figure 24. RTD allocated in the slot, adapted from [98].

Figure 25 shows the structure of a typical machine, indicating the location of the RTDs, the PD detection zone by coupling capacitors, and the PD activity in a region distant from the couplers.

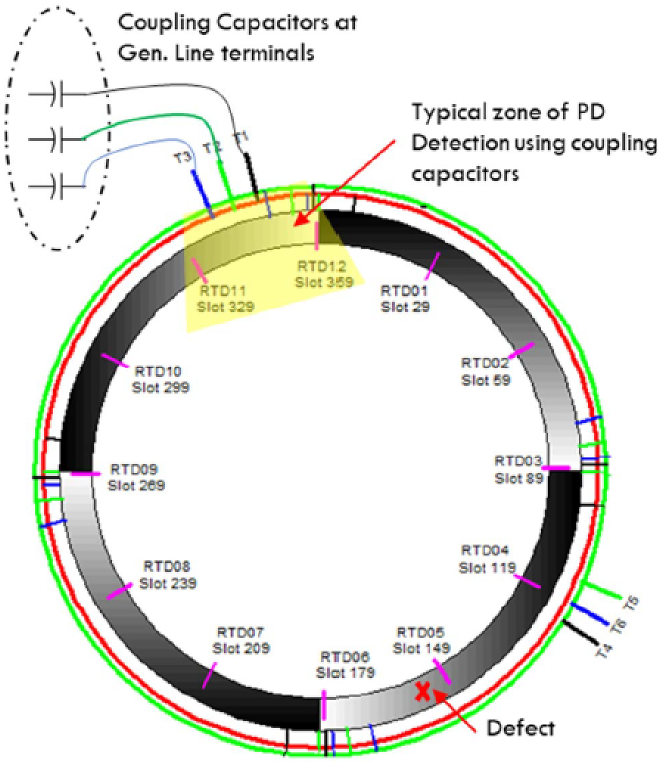

Figure 25. Typical structure of a monitoring system with RTDs [99].

In [99], online monitoring of a set of assets of the industry is realized, with data collection performed by 80 pF capacitive sensors installed at the terminals of each phase of the machines and with the aid of two RTDs per phase serving as antennas for the propagating PD pulses, according to the structure shown in Figure 25. The data analysis methodology uses a window of measurement of power dissipated by the PD on each phase and then defines severity levels to select the machines with significant damage. Although the methodology achieves a good coverage area, it can identify PDs by zones and not the exact location.

In [97], a data collection methodology that used the combination of capacitive sensors with RTDs and ground leakage current sensors to obtain a greater coverage of the signals from a hydro generator was presented. In the presented structure, the RTDs act as antennas for the propagation of pulses from PDs, since the magnitude of the pulses measured in the RTD can be an indicator of where the failure is occurring. Regarding the current sensor, the advantage is that it can be installed at ground potential, eliminating the problems of false PD readings due to incorrect mounting or poor quality of capacitive couplers. The study used the PRPD pattern to identify PD activity. Visual inspection is used to verify the results obtained by the PRPD pattern.

A case study for a gas turbine generator is presented in [98]. The methodology used capacitive sensors, RTDs, and corona probes to detect PDs. First, a sensitivity comparison was made between the capacitive sensors and the RTDs, where it was verified that in phase B, an RTD located three slots away from the coupling capacitor registered a charge of 10 nC while the capacitor registered 1 nC, for a PD source closer to the RTD. In a second moment, tests were realized to identify the zones of activity of PDs, comparing the measurements of RTDs with those of a corona probe, where the places of defects indicated by the RTDs and corona probe showed similar results. The identification of the PD source was done using PRPD patterns.

RTDs seem to be a good option as a complementary way to detect PDs. However, these sensors are designed to measure machine temperature, not to collect PD pulses. In addition, there is no current standard that indicates which guidelines must be followed for the use of RTDs in the measurement of PDs. For an adequate application of RTDs in PDs measuring, it is necessary to analyze the cabling used, since it can influence the transfer of signal power, since the pulse is attenuated due to the length and shielding of the conductors. Some conclusions obtained from online and offline tests realized by [100] on eight machine stators, which were not explained in the studies of [97–99], are important to consider in the use of RTDs for detecting of PDs, which are:

- In some cases, it is the RTD conductor, and not the RTD, which detects the PD, due to the path that the cabling takes through the stator;
- The reading of the magnitude of the PD is influenced by the shielding and the length of the conductors of the RTDs, since the tests showed that, for shielded conductors and long lengths, the magnitude of the measured PD is attenuated, making it difficult to interpret the severity level of the insulation defect;
- The data collected by RTDs did not correlate with the physical state of the insulation, nor with the reading of conventional sensors;
- Due to the path taken by the RTD conductor, pulses of different phases will propagate through the conductor, causing the overlap of clusters to occur, which in many cases makes it difficult to separate sources and noise;
- The actual position of the pulses relative to the phase reference is unknown, and the pulse polarity is lost when using HFCT to collect data from the RTD cabling.

5.4.2. Use of Software

In [101], online monitoring of the stator winding of a 10.5 kV turbo generator is discussed. The study presents a method for the interpretation of PD data collected from capacitive sensors and treated by the TGA-B instrument from the company IRIS Power. It was possible to determine the size and location of the defects only for coils near the stator terminals. The COMSOL software performed the simulation of cavity sizes and shapes in the winding isolation using finite elements, and PDViwe and PD ANALYZER-KSPEU software programs were developed to analyze and interpret the data. The methodology presented is innovative, but it is necessary to realize more tests to verify its consistency.

6. Suggested Improvements

During the survey of methodologies about PDs monitoring in rotating electrical machines, some gaps were found that need to be filled to make the detection process more reliable.

First, it was observed that most methodologies analyze the data without adopting a criterion to determine the levels of PD indicators.This happens because the vast majority of works are based on standards without considering the specific characteristics of the machines and operating environments. Thus, to define a machine acceptance criterion based on PD measurements, it is necessary to obtain a significant amount of test data from machines similar to the one under analysis to apply statistical methods or machine learning methods for threshold definition and winding condition classification.

Second, there are still few studies associated with the location of PDs in the stator winding, with a predominance of those using RTDs, as presented in the previous section. In the literature, no conclusive studies were found on the frequency range to which RTDs are sensitive or on the influence of the length of the RTDs conductors on PD measurements. Discussions about validation of PD signals measured using RTDs were also not found. There are also no current standards that indicate guidelines to be followed in the RTD approach to locate PDs. Each supplier of RTDs uses specific technologies to encapsulate the sensors, so it is concluded that the measurement by RTDs signals would be reliable only if characteristics such as frequency response, immunity to external noise, and characteristics of the conductors were known. Finally, the cables of RTDs usually run behind the end-winding, often being exposed, which leads to frequent breakages and sensor unavailability. As a conclusion, the use of RTDs to measure PDs may be promising, as long as a specific and known sensor design is used. The out-of-the-box use of RTDs provided by machine manufacturers does not guarantee that the sensors present adequate characteristics for the reliable measurement of PDs.

A third factor that is not widely addressed in the literature was the influence of the drive system on the detection of PDs, as these interfere with the detection either through the addition of background noise or by pulse amplification, in addition to the need to have a frequency reference for data analysis. Noise addition can be resolved by applying hardware- and software-based filters. For the question of pulse amplification, it is necessary to calibrate the instruments used in the detection of PDs. Concerning the reference frequency, the methodology used in [95] is an alternative, but other hardware topologies can be suggested to that end.

In addition to the challenges presented above, a maintenance system based on forecasting techniques, such as time series realization algorithms, was not found in the literature. This kind of system could help to predict the useful life of the winding insulation, allowing us to make the right decisions before failures occur.

Faced with the challenges, an online monitoring system that does not use intrusive methods for data collection, that identifies PDs autonomously in any machine and operating environment, and that has a system for predicting the useful life of the winding insulation is highly desirable.

7. Conclusions

In this study, a bibliographic review was realized on the subject of PDs in the context of rotating electrical machines to verify the current state of the methodologies used in the development of PD monitoring systems. The review aimed to better understand the structural concepts of machine winding insulation, define the types of PDs and how they occur, verify how measurements are made, which commercial equipments are present on the market, what types of sensors and topologies of installation are used, what techniques are applied to analyze the data, whether the influence of the drive system was considered, and how they physically locate the sources of PDs.

There are several commercial equipments for detecting PDs in generators and electric motors that employ consolidated and mature techniques. These pieces of equipment are distinguished mainly by the detection method, couplers (sensors), and frequency range. Equipment with smaller coupling capacitors (e.g., 80 pF) filter signals below 40 MHz analogically and present good immunity to low-frequency noise. On the other hand, this strategy makes it impossible to recognize PD events at relatively low frequencies. Equipment that applies filters using digital signal processing can use higher-value coupling capacitors and thus is not limited by analogic filters.

In the context of data analysis, machine learning techniques are gradually being introduced to identify PDs autonomously, without the need to have a specialist on standby to determine whether it is time to intervene in the operation of the machine. Furthermore, these algorithms are able to learn the behavior of the machine according to its characteristics, so that it is possible to identify the activity of PDs and set thresholds without relying on tests from different machines. In the literature, there are still few studies that analyze the influence of the drive system on the detection of PDs, use methods that address the location of PDs, present machine learning techniques for recognition and patterns, and use prediction techniques to estimate the remaining useful life of windings in electric machines. These are some of the current challenges to be addressed by the PD monitoring community.

The prospects for the development of an online monitoring system for the diagnosis of partial discharges in rotating machines through AI are encouraging and of great relevance for realizing the asset management of an industry. Automation using AI enables a robust and reliable management model due to the learning capacity that the algorithms have, making it possible to verify the condition of the machine insulation, and forecasting its remaining useful life.

Author Contributions: Conceptualization, J.d.S.C., F.F., R.d.R.L. and M.G.; methodology, J.d.S.C., F.F., R.d.R.L. and M.G.; validation, J.d.S.C., F.F., R.d.R.L. and M.G.; formal analysis, J.d.S.C., F.F., R.d.R.L. and M.G.; investigation, J.d.S.C.; resources, F.L.T., C.d.A.T., E.R.d.L. and M.G.; data curation, J.d.S.C.; writing—original draft preparation, J.d.S.C.; writing—review and editing, J.d.S.C., F.F., R.d.R.L. and M.G.; visualization, J.d.S.C., F.F., R.d.R.L. M.G., F.L.T., C.d.A.T. and E.R.d.L; supervision, M.G.; project administration, F.L.T., C.d.A.T., E.R.d.L. and M.G.; funding acquisition, F.L.T., C.d.A.T., E.R.d.L. and M.G. All authors have read and agreed to the published version of the manuscript.

Funding: Financial support from the Petrobras for both the University of Campinas and the School of Electrical and Computer Engineering University of Campinas is acknowledged.

Institutional Review Board Statement: Not applicable.

Informed Consent Statement: Not applicable.

Data Availability Statement: Not applicable.

Acknowledgments: The authors are thankful to Petrobras and Instituto Eldorado for the support given to developing this research.

Conflicts of Interest: The authors declare no conflict of interest.

References

1. Ritchie, H.; Roser, M.; Rosado, P. Energy. Our World in Data 2020. Available online: https://ourworldindata.org/energy (accessed on 3 October 2022).
2. OMICRON. Diagnostic Testing and Monitoring of Rotating Machines. Available online: https://www.omicronenergy.com/download/document/40CEA890-3E5B-447D-BEF5-51CBE544A6E0/ (accessed on 31 June 2022).
3. Wang, W.; Yan, L.; Wang, T.; Yu, H.; Han, Y.; Liu, X.; Zhang, N.; Wu, N. PD mechanism and pattern investigation for stator winding insulation of HV motors. In Proceedings of the 2016 IEEE International Conference on Mechatronics and Automation, Harbin, China, 7–10 August 2016, pp. 1232–1237. [CrossRef]
4. Fuangpian, P.; Suwanasri, T.; Suwanasri, C. Partial Discharge Severity Analysis Based on Repetition Rate, Amplitude and Gap Distance in MV Motor. In Proceedings of the 21st International Symposium on High Voltage Engineering, Budapest, Hungary, 26–30 August 2019, Németh, B., Ed.; Springer International Publishing: Cham, Switzerland, 2020; pp. 704–717.
5. Leffler, J.; Trnka, P. Failures of Electrical Machines—Review. In Proceedings of the 2022 8th International Youth Conference on Energy (IYCE), Eger, Hungary, 6–9 July 2022; pp. 1–4. [CrossRef]
6. He, M.; He, D. Deep Learning Based Approach for Bearing Fault Diagnosis. *IEEE Trans. Ind. Appl.* **2017**, *53*, 3057–3065. [CrossRef]
7. Zhang, W.; Li, X.; Ma, H.; Luo, Z.; Li, X. Universal Domain Adaptation in Fault Diagnostics With Hybrid Weighted Deep Adversarial Learning. *IEEE Trans. Ind. Inform.* **2021**, *17*, 7957–7967. [CrossRef]
8. IRIS Power. Partial Discharge Monitoring. Available online: https://irispower.com/monitoring/partial-discharge-pd-monitoring/ (accessed on 1 June 2022).
9. OMICRON. What Is Partial Discharge? Available online: https://www.omicronenergy.com/download/document/C032C0D6-ED64-4278-A8BA-CA7B2AC673A0/ (accessed on 1 June 2022).
10. Hassan, W.; Hussain, G.A.; Mahmood, F.; Amin, S.; Lehtonen, M. Effects of Environmental Factors on Partial Discharge Activity and Estimation of Insulation Lifetime in Electrical Machines. *IEEE Access* **2020**, *8*, 108491–108502. [CrossRef]
11. Khan, Q.; Refaat, S.S.; Abu-Rub, H.; Toliyat, H.A. Partial Discharge Modeling of Internal Discharge in Electrical Machine Stator Winding. In Proceedings of the 2020 IEEE Kansas Power and Energy Conference (KPEC), Manhattan, KS, USA, 13–14 July 2020; pp. 1–6. [CrossRef]

12. Stone, G. A perspective on online partial discharge monitoring for assessment of the condition of rotating machine stator winding insulation. *IEEE Electr. Insul. Mag.* **2012**, *28*, 8–13. [CrossRef]
13. Luo, Y.; Li, Z.; Wang, H. A Review of Online Partial Discharge Measurement of Large Generators. *Energies* **2017**, *10*, 1694. [CrossRef]
14. Vala, S.S.; Mirza, A.B.; Luo, F. A Review on Partial Discharge Phenomenon in Rotating Machines Operated Using WBG Motor Drives. In Proceedings of the 2022 IEEE Transportation Electrification Conference & Expo (ITEC), Haining, China, 28–31 October 2022; pp. 523–528. [CrossRef]
15. Stone, G.; Boulter, E.A.; Culbert, I.; Dhirani, H. *Electrical Insulation for Rotating Machines: Design, Evaluation, Aging, Testing, and Repair*, 1st ed.; Wiley-Blackwell: Piscataway, NJ, USA, 2004.
16. Kokkotis, A.; Seltzer-Grant, M.; Polley, A.; Barnwell, E. Advanced Analysis and Diagnostics for Remote Online PD Monitoring of HV Rotating Machines. In Proceedings of the 2018 IEEE International Conference on High Voltage Engineering and Application (ICHVE), Athens, Greece, 10–13 September 2018; pp. 1–4. [CrossRef]
17. Tremblay, R.; Hudon, C. Improved Requirements for Stress-Grading Systems at Hydro-Québec. In Proceedings of the Iris Rotating Machine Conference, San Antonio, TX, USA, 4–7 June 2007; pp. 1–6.
18. *IEC TS 60034-27:2006*; Rotating Electrical Machines–Part 27: Off-line Partial Discharges Measurements on the Stator Winding Insulation of Rotating Electrical Machines. IEC: Geneva, Switzerland, 2006; pp. 1–111.
19. *IEC 60034-27-1:2017*; Rotating Electrical Machines—Part 27-1: Off-Line Partial Discharge Measurements on the Winding Insulation. IEC: Geneva, Switzerland, 2017; pp. 1–133.
20. *IEEE Std 1434-2014 (Revision of IEEE Std 1434-2000)*; IEEE Guide for the Measurement of Partial Discharges in AC Electric Machinery. IEEE: Piscataway, NJ, USA, 2014; pp. 1–89. [CrossRef]
21. Stone, G.; Sasic, M. Twenty-five Years of Experience With On-line Partial Discharge Testing of Stator Windings. In Proceedings of the 12th INSUCON Conference, Birmingham, UK, 29–31 May 2013; pp. 152–157.
22. Franco, J.R.; Richards, M.; Seltzer-Grant, M. 8 Years Experience in Large-Scale Remote Partial Discharge Monitoring of HV Motors in an Oil and Gas Environment. In Proceedings of the 2019 IEEE Petroleum and Chemical Industry Committee Conference (PCIC), Vancouver, BC, Canada, 9–12 September 2019; pp. 23–32. [CrossRef]
23. Mitiche, I.; Morison, G.; Hughes-Narborough, M.; Nesbitt, A.; Boreham, P.; Stewart, B.G. Classification of partial discharge signals by combining adaptive local iterative filtering and entropy features. In Proceedings of the 2017 IEEE Conference on Electrical Insulation and Dielectric Phenomenon (CEIDP), Fort Worth, TX, USA, 22–25 October 2017; pp. 335–338. [CrossRef]
24. Stone, G.; Sedding, H.; Veerkamp, W. What Medium and High Voltage Stator Winding Partial Discharge Testing Can - And Can Not - Tell You. In Proceedings of the 2021 IEEE IAS Petroleum and Chemical Industry Technical Conference (PCIC), San Antonio, TX, USA, 13–16 September 2021; pp. 293–302. [CrossRef]
25. Dehlinger, N.; Stone, G. Surface partial discharge in hydrogenerator stator windings: Causes, symptoms, and remedies. *IEEE Electr. Insul. Mag.* **2020**, *36*, 7–18. [CrossRef]
26. Phloymuk, N.; Phumipunepon, N.; Pattanadech, N. Partial discharge behaviors of a surface discharge problem of the stator insulation for a synchronous machine. In Proceedings of the 2018 12th International Conference on the Properties and Applications of Dielectric Materials (ICPADM), Xi'an, China, 20–24 May 2018; pp. 385–388. [CrossRef]
27. Stone, G.; Sedding, H. Comparison of Low and High Frequency Partial Discharge Measurements on Stator Windings. In Proceedings of the NORD-IS 2019, Tampere, Finland, 12–14 June 2019; pp. 1–5.
28. Lachance, M.; Oettl, F. A Study of the Pulse Propagation Behavior in a Large Turbo Generator. In Proceedings of the 2020 IEEE Electrical Insulation Conference (EIC), Knoxville, TN, USA, 22 June–3 July 2020; pp. 434–439. [CrossRef]
29. Oettl, F.; Engelen, C.; Binder, E.; Kessler, T. A study of the propagation behaviour of partial discharge pulses in the high-voltage winding of hydro generators. *Elektrotech. Inftech* **2018**, *135*, 528–535. [CrossRef]
30. Stone, G.; Sedding, H.; Chan, C.; Wendel, C. Comparison of Low Frequency and High Frequency PD Measurements on Rotating Machine Stator Windings. In Proceedings of the 2018 IEEE Electrical Insulation Conference (EIC), San Antonio, TX, USA, 17–20 June 2018; pp. 349–352. [CrossRef]
31. Nair, R.P.; Vishwanath, S.B. Identification of Simultaneously Active PD Sources in Stator Insulation Using Variable Frequency Excitation. *IEEE Trans. Dielectr. Electr. Insul.* **2021**, *28*, 646–653. [CrossRef]
32. *IEC TS 60034-27-2:2012*; Rotating Electrical Machines-Part 27-2: On-Line Partial Discharge Measurements on the Stator Winding Insulation of Rotating Electrical Machines. IEC: Geneva, Switzerland, 2012; pp. 1–55.
33. Hudon, C.; Belec, M. Partial discharge signal interpretation for generator diagnostics. *IEEE Trans. Dielectr. Electr. Insul.* **2005**, *12*, 297–319. [CrossRef]
34. Lévesque, M.; Bélec, M.; Hudon, C.; Guddemi, C. The need for PD quantification based on the type of discharge sources. In Proceedings of the 2017 IEEE Electrical Insulation Conference (EIC), Baltimore, MD, USA, 11–14 June 2017; pp. 380–383. [CrossRef]
35. Caprara, A.; Ciotti, G.; Paschini, L. Analysis of the results of on-line Partial Discharge Monitoring and the impact of the maintenance actions on a 30 MVA synchronous generator. In Proceedings of the 2020 IEEE Electrical Insulation Conference (EIC), Knoxville, TN, USA, 22 June–3 July 2020; pp. 359–362. [CrossRef]

36. Sasic, M.; Sedding, H.; Stone, G.C. Distinguishing Between Phase to Ground, Phase to Phase and Cross-Coupled PD Signals in Stator Windings. In Proceedings of the 2021 IEEE Electrical Insulation Conference (EIC), Denver, CO, USA, 7–28 June 2021; pp. 393–396. [CrossRef]
37. Luo, Y.; Li, Z.; Chen, T. Experimental study of partial discharge pulses propagation in stator winding of hydro generator. In Proceedings of the 2017 IEEE 2nd Information Technology, Networking, Electronic and Automation Control Conference (ITNEC), Chengdu, China, 15–17 December 2017; pp. 773–777. [CrossRef]
38. Oettl, F.; Krueger, M.; Koltunowicz, K.W.; Badicu, L.; Gorgan, B. Partial Discharge Measurements on Rotating Machines—Experience and Innovation. Available online: https://www.omicronenergy.com/download/document/CA07C27B-ABCF-484C-B130-D6355100C296/ (accessed on 5 June 2022).
39. Gorgan, B.; Koltunowicz, W.; Zander, P. Temporary Monitoring of Stator Winding Insulation Using an Advanced PD System. In Proceedings of the 2020 International Conference on Diagnostics in Electrical Engineering (Diagnostika), Pilsen, Czech Republic, 1–4 September 2020; pp. 1–4. [CrossRef]
40. Koltunowicz, W.; Gorgan, B.; Broniecki, U.; Nadaczny, J.; Pawlik, B.; Cordova, J.; Barbadillo, D. Evaluation of Stator Winding Insulation Using a Synchronous Multi-Channel PD Technique. *IEEE Trans. Dielectr. Electr. Insul.* **2020**, *27*, 1889–1897. [CrossRef]
41. Stone, G.C.; Chan, C.; Sedding, H.G. Relative ability of UHF antenna and VHF capacitor methods to detect partial discharge in turbine generator stator windings. *IEEE Trans. Dielectr. Electr. Insul.* **2015**, *22*, 3069–3078. [CrossRef]
42. C.Hatiegan.; Padureanu, I.; Jurcu, M.R.; Biriescu, M.; Raduca, M.; Dilertea, F. The evaluation of the insulation performances of the stator coil for the high power vertical synchronous hydro-generators by monitoring the level of partial discharges. *Electr. Eng.* **2017**, *99*, 1013–1020. [CrossRef]
43. *IEEE Std 3004.8-2016*; IEEE Recommended Practice for Motor Protection in Industrial and Commercial Power Systems. IEEE: Piscataway, NJ, USA, 2017; pp. 1–163. [CrossRef]
44. Lachance, M.; Sze, M.; Oettl, F.; Desrochers, D. Limitations of magnitude guidelines for PD Measurements on Stator Windings. In Proceedings of the 2021 IEEE Electrical Insulation Conference (EIC), Denver, CO, USA, 7–28 June 2021; pp. 424–428. [CrossRef]
45. Stone, G.; Sedding, H.; Chan, C.; Wendel, C. Progress in Interpreting On-line Partial Discharge Test Results from Motor AND Generator Stator Windings. In Proceedings of the CIGRE 2016, Paris, France, 21–26 August 2016; pp. 1–7.
46. IPEC. High Frequency Current Transformer (HFCT). Available online: https://ipec.co.uk/pd-products/high-frequency-current-transformer-hfct/ (accessed on 1 August 2022).
47. HVPD. High Voltage Coupling Capacitor (HVCC). Available online: https://www.hvpd.co.uk/hvcc/ (accessed on 1 August 2022).
48. OMICRON. MPD 800 Product Information Brochure. Available online: https://www.omicronenergy.com/pt/produtos/mpd-800/ (accessed on 1 August 2022).
49. IRIS Power. Iris Power TGA. Available online: https://irispower.com/wp-content/uploads/2022/02/TGA-Iris-Qualitrol-Brochure-V1-10-21.pdf (accessed on 1 August 2022).
50. IRIS Power. PDA-IV—PARTIAL DISCHARGE MONITORING. Available online: https://irispower.com/products/pda-iv/ (accessed on 1 August 2022).
51. doble. doblePRIME PD-Guard. Available online: https://www.doble.com/product/partial-discharge-monitor/ (accessed on 1 August 2022).
52. OMICRON. MONGEMO. Available online: https://www.omicronenergy.com/en/products/mongemo/ (accessed on 1 August 2022).
53. OMICRON. MONTESTO 200. Available online: https://www.omicronenergy.com/en/products/montesto-200/ (accessed on 1 August 2022).
54. HPVD. HVPD Kronos Permanent Monitor. Available online: https://www.hvpd.co.uk/kronos/ (accessed on 1 August 2022).
55. ALTANOVA GROUP SRL. PD Hub. Available online: https://www.altanova-group.com/en/products/partial-discharge-tests/acquisition-units/pd-monitoring-systems (accessed on 1 August 2022).
56. Megger. Partial Discharge Testing from Power Diagnostix. Available online: https://media.megger.com/mediacontainer/medialibraries/meggerse/images/produktkataloger/powerdiagnostix_catalogue_2020_en_digital.pdf (accessed on 1 August 2022).
57. ELETRONS LIVRES TECNOLOGIA E SERVICOS LTDA. IMA-DP. Available online: https://eletronslivres.com.br/wp-content/uploads/2021/06/Instrumentacao-para-Monitoramento-e-Analise-de-Descargas-Parciais-IMA-DP.pdf (accessed on 1 August 2022).
58. Amperis. Partial discharge detector PXDP-II. Available online: https://amperis.com/en/products/partial-discharge-detector/pxdp2/ (accessed on 1 August 2022).
59. Sparks Instruments. Escort TMS-6141 Partial Discharge Monitor. Available online: https://sparksinstruments.com/product/escort-tms-6141-partial-discharge-monitor/ (accessed on 1 August 2022).
60. PDS. PDS Product Guide. Available online: https://pdicus.com/wp-content/uploads/2018/11/2018-Catalog-Rev-G-Letter-Size.pdf (accessed on 1 August 2022).
61. Dynamics Ratings. DRPD-15 Portable Partial Discharge Analyzer. Available online: https://www.dynamicratings.com/products/drpd15-portable-pd-analyzer/ (accessed on 5 July 2022).
62. CanalEnergia. Cepel conquista prêmio internacional com sistema IMA-DP. Available online: https://canalenergia.com.br/noticias/53062341/cepel-conquista-premio-internacional-com-sistema-ima-dp (accessed on 5 July 2022).

63. Haq, S.U.; Thirugnanasam, M.; Dickens, K.; Tariq, H. What Should You Know Before Acquiring Partial Discharge on High Voltage Motors and Generators. In Proceedings of the 2021 IEEE IAS Petroleum and Chemical Industry Technical Conference (PCIC), San Antonio, TX, USA, 13–16 September 2021; pp. 247–256. [CrossRef]
64. Stone, G.C.; Chan, C.; Sedding, H.G. On-line partial discharge measurement in hydrogen-cooled generators. In Proceedings of the 2016 IEEE Electrical Insulation Conference (EIC), Montreal, QC, Canada, 19–22 June 2016; pp. 194–197. [CrossRef]
65. Warren, V.; Stone, G.; Sedding, H. Partial Discharge Testing: A Progress Report. In Proceedings of the IRMC 2021, Buenos Aires, Argentina, 21–24 June 2021; pp. 1–9.
66. Blokhintsev, I.; Kozusko, J.; Oberer, B.; Anzaldi, D. Simple statistical approach presenting Partial Discharge data in large pool of MV motors in continuous and remote PD monitoring system. In Proceedings of the 2017 IEEE Electrical Insulation Conference (EIC), Baltimore, MD, USA, 11–14 June 2017; pp. 339–343. [CrossRef]
67. Syafruddin, H.; Lubis, D.T. Detection and Analysis of Partial Discharge Online System in Generator of Gas Turbine : A case study. In Proceedings of the 2020 4rd International Conference on Electrical, Telecommunication and Computer Engineering (ELTICOM), Medan, Indonesia, 3–4 September 2020; pp. 23–28. [CrossRef]
68. Foxall, M.; Giussani, R.; Seltzer-Grant, M.; Sheen, B. On-Line Partial Discharge Condition Monitoring Strategies for Oil and Gas High Voltage Assets Optimisation. In Proceedings of the 2018 Petroleum and Chemical Industry Conference Europe (PCIC Europe), Antwerp, Belgium, 5–7 June 2018; pp. 1–8. [CrossRef]
69. Jitjing, P.; Suppitaksakul, C.; Boonphen, W. Partial Discharge Signals Detecting and Preventive Maintenance Planning for 21 kV Generator Case Study of a Generator at the Combined cycle Power Plant of Ratchaburi Power Company Limited. In Proceedings of the 2018 15th International Conference on Electrical Engineering/Electronics, Computer, Telecommunications and Information Technology (ECTI-CON), Chiang Rai, Thailand, 18–21 July 2018; pp. 41–44. [CrossRef]
70. Zatsarinnaya, Y.; Suslov, K.; Danilin, A. Assessment of the Technical Condition of Turbogenerators by Partial Discharges. In Proceedings of the 2020 International Ural Conference on Electrical Power Engineering (UralCon), Chelyabinsk, Russia, 22–24 September 2020; pp. 225–229. [CrossRef]
71. McGreevy, D.; Giussani, R.; Seltzer-Grant, M.; Singh, A.; Patel, A.; Calladine, S.; Gibb, G. Deployment of an online partial discharge monitoring system for power station with focus on gas turbine generators. In Proceedings of the 2017 INSUCON—13th International Electrical Insulation Conference (INSUCON), Birmingham, UK, 16–18 May 2017; pp. 1–5. [CrossRef]
72. Lelio, R.; Duarte, R.; Vilhena, P.; Brasil, F. Manutenção Preditiva na uhe Balbina. In Proceedings of the CIGRE, Rio De Janeiro, Brazil, 23–25 May 2016, pp. 1–8.
73. Hassan, W.; Mahmood, F.; Hussain, G.A.; Amin, S.; Kay, J.A. Feature Extraction of Partial Discharges During Multiple Simultaneous Defects in Low-Voltage Electric Machines. *IEEE Trans. Instrum. Meas.* **2021**, *70*, 1–10. [CrossRef]
74. Hassan, W.; Mahmood, F.; Hussain, G.A.; Amin, S. Risk assessment of low voltage motors based on PD measurements and insulation diagnostics. *Measurement* **2021**, *176*, 109151. [CrossRef]
75. Araújo, R.C.F.; de Oliveira, R.M.S.; Barros, F.J.B. Automatic PRPD Image Recognition of Multiple Simultaneous Partial Discharge Sources in On-Line Hydro-Generator Stator Bars. *Energies* **2022**, *15*, 326. [CrossRef]
76. Araújo, R.C.F.; de Oliveira, R.M.S.; Brasil, F.S.; Barros, F.J.B. Novel Features and PRPD Image Denoising Method for Improved Single-Source Partial Discharges Classification in On-Line Hydro-Generators. *Energies* **2021**, *14*, 3267. [CrossRef]
77. Oliveira, R.M.S.; Araújo, R.C.F.; Barros, F.J.B.; Segundo, A.P.; Zampolo, R.F.; Fonseca, W.; Dmitriev, V. A System Based on Artificial Neural Networks for Automatic Classification of Hydro-generator Stator Windings Partial Discharges. *J. Microwaves Optoelectron. Electromagn. Appl.* **2017**, *16*, 628–645. [CrossRef]
78. Pardauil, A.C.N.; Nascimento, T.P.; Siqueira, M.R.S.; Bezerra, U.H.; Oliveira, W.D. Combined Approach Using Clustering-Random Forest to Evaluate Partial Discharge Patterns in Hydro Generators. *Energies* **2020**, *13*, 5992. [CrossRef]
79. Carvalho, A.T.; Amorim, H.P.; Cunha, C.F.C.; Rodrigues, T.B.; Brasil, F.S.; Vilhena, P.R.M.; Carvalho, D.S. Virtual instrumentation for Partial Discharge monitoring. In Proceedings of the 2017 IEEE Electrical Insulation Conference (EIC), Baltimore, MD, USA, 11–14 June 2017; pp. 173–176. [CrossRef]
80. Landeira, V.A.R.; Argolo, D.L.; Amorim, H.P.; Carvalho, A.T. Instrumentation for Monitoring and Analysis of Partial Discharges: Viewer and Report Generator. In Proceedings of the 2018 IEEE International Conference on High Voltage Engineering and Application (ICHVE), Athens, Greece, 10–13 September 2018; pp. 1–4. [CrossRef]
81. Ortego, J.; Arcones, E.; Vera, C.; Álvarez, F.; Garnacho, F.; Khamlichi, A. Processing techniques applied to partial discharge measuring in rotating machines. In Proceedings of the 2020 IEEE 3rd International Conference on Dielectrics (ICD), Valencia, Spain, 5–31 July 2020; pp. 898–901. [CrossRef]
82. Lévesque, M.; Amyot, N.; Hudon, C.; Bélec, M.; Blancke, O. Improvement of a Hydrogenerator Prognostic Model by using Partial Discharge Measurement Analysis. In Proceedings of the Annual Conference of the Prognostics and Health Management Society 2017, St. Petersburg, FL, USA, 2–5 October 2017; Volume 9, pp. 1–8.
83. Seri, P.; Ghosh, R.; Montanari, G.C. An Unsupervised Approach to Partial Discharge Monitoring in Rotating Machines: Detection to Diagnosis With Reduced Need of Expert Support. *IEEE Trans. Energy Convers.* **2021**, *36*, 2485–2492. [CrossRef]
84. Herath, H.; Kumara, J.; Fernando, M.; Bandara, K.; Serina, I. Comparison of supervised machine learning techniques for PD classification in generator insulation. In Proceedings of the 2017 IEEE International Conference on Industrial and Information Systems (ICIIS), Peradeniya, Sri Lanka, 15–16 December 2017; pp. 1–6. [CrossRef]

85. Hudon, C.; Lévesque, M.; Kokoko, O.; Amyot, N.; Zemouri, R. Automatic Classification of 2D Partial Discharge from Generator On-Line Measurement. In Proceedings of the 2021 IEEE Electrical Insulation Conference (EIC), Denver, CO, USA, 7–28 June 2021; pp. 8–12. [CrossRef]
86. Zemouri, R.; Lévesque, M.; Amyot, N.; Hudon, C.; Kokoko, O.; Tahan, S.A. Deep Convolutional Variational Autoencoder as a 2D-Visualization Tool for Partial Discharge Source Classification in Hydrogenerators. *IEEE Access* **2020**, *8*, 5438–5454. [CrossRef]
87. Zemouri, R.; Lévesque, M.; Amyot, N.; Hudon, C.; Kokoko, O. Deep Variational Autoencoder: An Efficient Tool for PHM Frameworks. In Proceedings of the 2020 Prognostics and Health Management Conference (PHM-Besançon), Besancon, France, 4–7 May 2020; pp. 235–240. [CrossRef]
88. Kokoko, O.; Hudon, C.; Lévesque, M.; Amyot, N.; Zemouri, R. Comparison of an Automatic Classification of Partial Dischage Patterns for Large Hydrogenerator. In Proceedings of the 2021 IEEE International Conference on Prognostics and Health Management (ICPHM), Detroit, MI, USA, 7–9 June 2021; pp. 1–6. [CrossRef]
89. Geron, A. *Hands-On Machine Learning with Scikit-Learn & TensorFlow: Concepts, Tools, and Techniques to Build Intelligent Systems*, 1st ed.; O'REILLY: Sebastopol, CA, USA, 2017.
90. Stone, G.C.; Sedding, H.G.; Chan, C. Experience with on-line partial discharge measurement in high voltage inverter fed motors. In Proceedings of the 2016 Petroleum and Chemical Industry Technical Conference (PCIC), Philadelphia, PA, USA, 19–22 September 2016; pp. 1–7. [CrossRef]
91. Hassan, W.; Mahmood, F.; Andreotti, A.; Pagano, M.; Pagano, F. Influence of Voltage Harmonics on Partial Discharge Diagnostics in Electric Motors Fed by Variable-Frequency Drives. *IEEE Trans. Ind. Electron.* **2021**, *69*, 10605–10614.
92. Montanari, G.C.; Seri, P.; Hebner, R. Type Of Supply Waveform, Partial Discharge Behavior And Life Of Rotating Machine Insulation Systems. In Proceedings of the 2018 IEEE International Power Modulator and High Voltage Conference (IPMHVC), Jackson, WY, USA, 3–7 June 2018; pp. 176–179.
93. Stone, G.; Sedding, H.; Chan, C. Experience With Online Partial-Discharge Measurement in High-Voltage Inverter-Fed Motors. *IEEE Trans. Ind. Appl.* **2018**, *54*, 866–872. [CrossRef]
94. Stone, G.; Sedding, H. Case Studies in On-Line Measurement of PD in Motors Fed by Voltage Source PWM Drives. In Proceedings of the ICPADM 2015, Sydney, Australia, 19–22 July 2015; pp. 1–5.
95. Sedding, H.G.; Stone, G.C.; Chan, C. Measuring partial discharge on operating motors with VS-PWM drives. In Proceedings of the 2017 INSUCON—13th International Electrical Insulation Conference (INSUCON), Birmingham, UK, 16–18 May 2017; pp. 1–6. [CrossRef]
96. Stone, G.; Sedding, H. Detection of stator winding stress relief coating deterioration in conventional and inverter fed motors and generators. In Proceedings of the 2016 International Conference on Condition Monitoring and Diagnosis (CMD), Xi'an, China, 25-28 September 2016; pp. 270–273. [CrossRef]
97. Kuppuswamy, R.; Rainey, S. Facilitating Proactive Stator Winding Maintenance Using Partial Discharge Patterns. In Proceedings of the 2018 IEEE Electrical Insulation Conference (EIC), San Antonio, TX, USA, 17–20 June 2018; pp. 566–571. [CrossRef]
98. Kuppuswamy, R.; Rainey, S. Synthesis of Experiences using Resistive Temperature Detectors (RTD) as PD Sensors for Detecting and Locating Electrical Defects inside Generator Stator Windings. In Proceedings of the 2019 IEEE Electrical Insulation Conference (EIC), Calgary, AB, Canada, 16–19 June 2019; pp. 405–409. [CrossRef]
99. Kuppuswamy, R. Method to Profile the Maintenance Needs of a Fleet of Rotating Machine Assets using Partial Discharge Data. In Proceedings of the 2020 IEEE Electrical Insulation Conference (EIC), Knoxville, TN, USA, 22 June–3 July 2020; pp. 286–289. [CrossRef]
100. Campbell, S.; Stone, G. Investigations into the use of temperature detectors as stator winding partial discharge detectors. In Proceedings of the Conference Record of the 2006 IEEE International Symposium on Electrical Insulation, Toronto, ON, Canada, 11–14 June 2006; pp. 369–375. [CrossRef]
101. Baboraik, A.M.; Usachev, A.E.; Ali, Z.M. A New Proposed Method for Interpretation On-line Partial Discharge Measurements Data of Turbine Generator. *J. Electr. Eng. Technol.* **2020**, *15*, 1301–1311. [CrossRef]